



Original research article

Cellular fate decisions in the developing female anteroventral periventricular nucleus are regulated by canonical Notch signaling



Matthew J. Biehl^a, Kerim B. Kaylan^b, Robert J. Thompson^a, Rachel V. Gonzalez^a, Karen E. Weis^a, Gregory H. Underhill^b, Lori T. Raetzman^{a,*}

^a Department of Molecular and Integrative Physiology, University of Illinois at Urbana-Champaign, Urbana, IL 61801, United States

^b Department of Bioengineering, University of Illinois at Urbana-Champaign, Urbana, IL 61801, United States

ARTICLE INFO

Keywords:

Notch
AVPV
Tyrosine hydroxylase
Differentiation
Neurogenesis
Gliogenesis

ABSTRACT

The hypothalamic anteroventral periventricular nucleus (AVPV) is the major regulator of reproductive function within the hypothalamic-pituitary-gonadal (HPG) axis. Despite an understanding of the function of neuronal subtypes within the AVPV, little is known about the molecular mechanisms regulating their development. Previous work from our laboratory has demonstrated that Notch signaling is required in progenitor cell maintenance and formation of kisspeptin neurons of the arcuate nucleus (ARC) while simultaneously restraining POMC neuron number. Based on these findings, we hypothesized that the Notch signaling pathway may act similarly in the AVPV by promoting development of kisspeptin neurons at the expense of other neuronal subtypes. To address this hypothesis, we utilized a genetic mouse model with a conditional loss of *Rbpj* in *Nkx2.1* expressing cells (*Rbpj* cKO). We noted an increase in cellular proliferation, as marked by Ki-67, in the hypothalamic ventricular zone (HVZ) in *Rbpj* cKO mice at E13.5. This corresponded to an increase in general neurogenesis and more TH-positive neurons. Additionally, an increase in OLIG2-positive early oligodendrocytic precursor cells was observed at postnatal day 0 in *Rbpj* cKO mice. By 5 weeks of age in *Rbpj* cKO mice, TH-positive cells were readily detected in the AVPV but few kisspeptin neurons were present. To elucidate the direct effects of Notch signaling on neuron and glia differentiation, an in vitro primary hypothalamic neurosphere assay was employed. We demonstrated that treatment with the chemical Notch inhibitor DAPT increased *mKi67* and *Olig2* mRNA expression while decreasing astroglial *Gfap* expression, suggesting Notch signaling regulates both proliferation and early glial fate decisions. A modest increase in expression of TH in both the cell soma and neurite extensions was observed after extended culture, suggesting that inhibition of Notch signaling alone is enough to bias progenitors towards a dopaminergic fate. Together, these data suggest that Notch signaling restricts early cellular proliferation and differentiation of neurons and oligodendrocytes both in vivo and in vitro and acts as a fate selector of kisspeptin neurons.

1. Introduction

Development and patterning of the ventral diencephalon is dependent upon a concert of transcription factors in order to acquire regional identity (Ferran et al., 2015). As each specific region is formed, it begins producing cellular subtypes with distinct neuropeptides required for it to perform its functions (Yee et al., 2009). These collections of neuronal cell bodies are named hypothalamic nuclei and each contribute a unique role in regulating whole body homeostasis (Altman and Bayer, 1978). In particular, hypothalamic control of reproduction is regulated within the anterior portion of the hypothalamus, along the third ventricle (3V) in the arcuate nucleus and in the anteroventral periventricular nucleus (AVPV) (Simerly et al., 1985). This is performed by a population of

neurons producing the kisspeptin peptide, which is a strong activator of gonadotropin releasing hormone (GnRH) release to the anterior pituitary (Han et al., 2005). GnRH release is also potentially inhibited by dopamine produced by neurons expressing the enzyme tyrosine hydroxylase (TH) (Liu and Herbison, 2013). Interestingly, it has been shown that most kisspeptin expressing neurons co-express TH, whereas a subset of TH-positive neurons do not co-express kisspeptin, suggesting the importance for the finely tuned balance of each of these neuronal subpopulations in release of GnRH and the subsequent LH surge (Clarkson and Herbison, 2011). While numerous studies have focused on the function of these subpopulations within the AVPV, it still remains unclear the molecular mechanisms involved in both their differentiation from a common progenitor pool, as well as signals which instruct them

* Correspondence to: University of Illinois at Urbana-Champaign, 542 Burrill Hall 407 S. Goodwin Avenue, Urbana, IL 61801, United States.
E-mail address: raetzman@life.illinois.edu (L.T. Raetzman).

to express their unique neuropeptide profile. Only a few studies, most characterizing the development of TH- or ER α -positive mature cells, have been conducted (Bodo et al., 2006; Chakraborty et al., 2005).

Neurogenesis within the developing murine hypothalamus occurs primarily between E11.5 and E14.5, and gliogenesis following occurring from roughly E14.5–E19.5 (Marsters et al., 2016a, 2016b). Proper gliogenesis has been established to be critical for regulation of multiple processes within the hypothalamus. Namely, they can directly respond to circulating metabolic cues and modulate neuronal activity in the feeding centers of the brain (Horvath et al., 2010; Le Foll et al., 2014). Additionally, astrocytes have also recently been hypothesized to be involved in *de novo* synthesis of steroids, hinting at a role in central control of reproduction as well (Micevych et al., 2003). Finally, oligodendrocytes function to myelinate neurons throughout the brain in order to promote their rapid response to an ever changing environment (Melcangi et al., 1988). Multiple developmental signaling pathways have been implied in glial differentiation, many of which are also involved in hypothalamic specification and neurogenesis (Nery et al., 2001; Peng et al., 2012). For instance, the Sonic hedgehog (SHH) signaling pathway has been shown not only to be involved in early hypothalamic patterning and neurogenesis, but also promotes astrocytes and oligodendrocytes later in development via upregulation of *Olig2* and *Pdgfra*, two factors necessary for oligodendrocyte specification (Alvarez-Bolado et al., 2012; Nery et al., 2001). However, the role of other pathways in gliogenesis is relatively unexplored.

Near the end of embryogenesis, tanycytes, a specialized radial glia-like cell found within the hypothalamic ventricular zone (HVZ), appear (Altman and Bayer, 1978). They act as a source of stem cells in the postnatal period as well as providing information to mature cells within the parenchyma (Duncan et al., 2015; Robins et al., 2013). Given their relatedness to other radial glia, these specialized stem cells have been shown to robustly express *Gfap* as well as additional identifying transcription factors (Campbell et al., 2017; Walsh et al., 1978). Tanycytes have been most carefully studied in the tuberal hypothalamus but they are also present in the rostral periventricular region of the 3 V that gives rise to the AVPV (García et al., 2003; Salgado et al., 2014).

Ependymal cells are also found lining the 3 V and these cells likely arise from a common *Rax1* dependent lineage shared with tanycytes (Miranda-Angulo et al., 2014). Ciliated ependymal cells are important for movements of cerebral spinal fluid through the ventricle. These cells serve both a structural role to allow for the 3 V to maintain its integrity as well as a conduit to allow for rapid adjustments to whole body homeostasis depending on physiological need (De los Angeles García et al., 2003). The transcription factor FOXJ1 is known to be necessary to derive ependymal cells from progenitors in the lateral ventricles (Jacquet et al., 2009) and it continues to be expressed in these cells in the 3 V, although little attention has been given to the 3 V in the region of the AVPV (Miranda-Angulo et al., 2014; Yu et al., 2008).

One signaling pathway that has been shown to play a critical role in neuronal differentiation within the developing ventral diencephalon is the Notch signaling pathway (Chapouton et al., 2011). Notch signaling is an evolutionarily conserved cell-to-cell signaling pathway involved in progenitor maintenance, differentiation, fate choice, and patterning throughout the body (Lu et al., 2016; Okigawa et al., 2014). Classically, Notch signaling maintains progenitor cells through complexing with the co-activator RBPJ-K, among others, to activate of *Hes* family genes (de la Pompa et al., 1997). Typically, differentiation is prevented during high levels of *Hes* expression via active repression of proneural genes such as *Mash1* (Casarosa et al., 1999). Additionally, Notch signaling acts as a fate selector during development, such that active signaling may play a role in biasing an undifferentiated progenitor cell to adopt a specific cellular sub-fate (Ramamany and Lenka, 2010). Previous work from our laboratory has shown that loss of RBPJ-K results in progenitor cell loss and premature differentiation of *Pomc* expressing

neurons (Aujla et al., 2013). Interestingly, Notch signaling is also necessary during development to give rise to kisspeptin neurons of the ARC, suggesting its role in later fate decisions as well (Biehl and Raetzman, 2015). We have also previously shown that active Notch signaling has the capability to promote premature gliogenesis and tanycyte specification within the ARC (Aujla et al., 2013). Additionally, in vitro studies have shown that inhibition of Notch signaling in human embryonic stem cells coupled with treatment of brain derived neurotrophic factor (BDNF) is sufficient to induce differentiation of neurons of an ARC phenotype, namely POMC, NPY, and dopaminergic neurons (Wang et al., 2014). While these phenomena have been observed in other regions of the brain and in vitro, it has yet to be shown the role Notch signaling has on development and cellular fate choices specifically within the AVPV.

The goal of the current study is to further our understanding of the development of each of the aforementioned cellular subtypes within the AVPV. We hypothesized that the Notch signaling pathway would both regulate cellular proliferation as well as early and late fate decisions within the AVPV. To address this hypothesis, we utilized a conditional knockout of *Rbpj* (*Rbpj* cKO) in *Nkx2.1* positive cells of the developing rostral ventral diencephalon. Additionally, we acutely manipulated Notch signaling in a pure population of hypothalamic progenitor cells in vitro. We report that loss of canonical Notch signaling does not affect SOX2-positive progenitor maintenance. Interestingly, loss of Notch signaling promotes cellular proliferation in vivo and in vitro. Active Notch signaling also appears to restrain TH-neuron number and OLIG2-positive parenchymal oligodendrocytic precursors in vivo and to some extent in vitro, while also being necessary for development of kisspeptin neurons of the AVPV. Taken together, these data suggest that Notch signaling is a critical controller of cellular proliferation, neurogenesis and gliogenesis, but is not involved in progenitor cell maintenance during development within the AVPV.

2. Materials and methods

2.1. Mice

RBPJ- κ conditional knock-out (*Rbpj* cKO) mice were generated using established genetic mouse models. *Rbpj*^{tm1Hon} (*Rbpj*- κ fl) mice provided by Dr. Tasuku Honjo (Kyoto University, Japan) (Tanigaki et al., 2004) were bred to C57BL/6J-Tg(Nkx2-1-cre)2Sand/J (Nkx2.1-cre) mice (Kusakabe et al., 2006) purchased from Jackson Laboratories to generate *Rbpj* cKO mice. B6. Cg-Gt(Rosa)26Sor^{tm9(CAG-tdTomato)Hze/J} (*Rosa*^{tdTomato} fl) mice (Madisen et al., 2010) were also purchased from Jackson Laboratories and mated to Nkx2.1-cre mice to lineage trace *Nkx2.1* expressing cells. CD-1 mice (Charles Rivers Laboratories, USA) of mixed sexes were used to generate hypothalamic neurospheres. To genotype, tail biopsies were collected and DNA was extracted either via salt-out or HotSHOT method (Madisen et al., 2010; Miller et al., 1988; Truett et al., 2000). PCR was performed on DNA utilizing primer sets previously described or from Jackson Laboratory's online database (Aujla et al., 2013; Goldberg et al., 2011). Breeding colonies were maintained in a facility with a 12-h light/dark cycle at the University of Illinois at Urbana Champaign (UIUC). All protocols were approved by the UIUC Institutional Animal Care and Use Committee.

2.2. Tissue collection

Rbpj^{fl/fl}; Nkx2.1-cre^{+/+} (*Rbpj* control) or *Rbpj*^{fl/fl}; Nkx2.1-cre^{+/cre} (*Rbpj* cKO) mice were collected on embryonic day (E)13.5 (both sexes) or the day of birth (P0) (females only) and fixed for 1 h at room temperature (E13.5) or overnight at 4 °C (P0) in 3.7% formaldehyde solution (Sigma-Aldrich, USA) diluted in phosphate-buffered saline (PBS). The day a visible plug was detected was determined as E0.5. Tissue was then dehydrated through graded ethanols, methyl salicylate,

and embedded in paraffin wax. Serial sagittal (E13.5) or coronal sections (P0) (6 μ m) were collected and two or three sequential sections were mounted on charged slides for histological analysis. *Rbpj* control and cKO brains collected at P35 were collected from mice perfused with 4% PFA (Fisher Scientific, USA) dissolved in PBS, cryoprotected at 4 °C in 30% sucrose solution in PBS and then snap frozen in O.C.T. compound (TissueTek, CA, USA). Serial coronal sections (10 μ m) were collected and mounted on charged slides for histological analysis as similarly described above. For lineage tracing, *Nkx2.1-cre^{+/cre}* mice were mated to *Rosa^{tdTomato}* floxed mice and collected on E13.5. Embryos were fixed for 1 h at room temperature in 4% PFA, cryoprotected in 30% sucrose solution in PBS and snap frozen in O.C.T. compound. 10 μ m serial sagittal sections were collected and mounted as described above.

2.3. Immunohistochemistry

To observe gross morphology at E13.5 or P0, sections were deparaffinized, washed, stained with Hematoxylin Stain 3 (Fisher Scientific, USA) followed by staining with Eosin Y Solution with Phloxine (Sigma-Aldrich, MO, USA), washed, and mounted with Permount (Fisher Scientific, USA). For fluorescent microscopy, sections were deparaffinized, washed, and boiled in citrate solution (10 mM, pH 6.0). Following antigen retrieval, slides were blocked in blocking solution (5% normal donkey serum, 3% bovine serum albumen and 0.5% Triton-X100 diluted in sterile PBS). Frozen sections were thawed, fixed for 10 min in 4% PFA, washed in PBS, and blocked with identical solutions. Following blocking, antibody was incubated on tissue sections overnight at 4 °C diluted in appropriate blocking solution. Primary antibodies used were raised against the following peptides: tyrosine hydroxylase (TH) (AB152 1:1500; Millipore, MA, USA), SOX2 (AB5603 1:5000; Millipore, MA, USA), SOX9 (AB5535 1:1000; Millipore, MA, USA), ER α (06–935 1:1000; Millipore, MA, USA), Ki67 (550609 1:1000; BD Pharmingen, CA, USA), kisspeptin (Kp10) (AB9754 1:1500; Millipore, MA, USA), GFAP (RB-087-A1 1:250; Thermo Fisher Scientific, MA, USA) OLIG2 (MABN50 1:300; Millipore, MA, USA), FOXJ1 (14–9965 1:1:500; Affymetrix, CA, USA), HuC/D (A-21271 1:250; Molecular Probes, OR, USA), RBPJ (5313 1:2500, Cell Signaling, MA, USA). Slides were then incubated with biotin-conjugated rabbit (TH, SOX2, SOX9, ER α , GFAP, RBPJ) or mouse (Ki67, OLIG2, FOXJ1, HuC/D) secondary antibody (E13.5, P0) diluted in blocking solution for one hour at room temperature. Slides were then washed and incubated with streptavidin conjugated Cy3. Frozen sections were incubated with Cy3-conjugated rabbit (TH, Kp10, GFAP) for one hour at room temperature. Secondary and tertiary antibodies were purchased from Jackson ImmunoResearch (PA, USA) and all were used at a concentration of 1:200. Slides were mounted with mounting media containing 4',6-diamidino-2-phenylindole (DAPI, 1:1000; Sigma-Aldrich, MO, USA). Cell death via apoptosis was assessed via terminal deoxynucleotidyl transferase biotin-DUTP nick end labeling (TUNEL) method using the in situ cell death detection kit (Roche, IN, USA) according to manufacturer's protocol. Slides were then visualized at either 100 \times or 200 \times using a Leica DM2560. Images were taken using a Retiga 2000R color camera and acquired using Q-Capture software (Q-Imaging, Surrey, Canada). Images were processed using Adobe Photoshop CS6 (Adobe, CA, USA) and cells counts were quantified using ImageJ software (NIH, MD, USA).

2.4. In situ hybridization

Slides were deparaffinized, washed, permeabilized, digested with Proteinase-K, acetylated, and incubated in hybridization solution (55 °C). Probes for either *Notch1*, *Notch2*, *Hes1*, *Hes5*, *Mash1*, and *Shh* (Aujla et al., 2015, 2013) were all diluted 1:100 and linearized with appropriate enzymes and transcribed with polymerase in the presence

of digoxigenin-labeled nucleotides. Labeled probes were denatured at 95 °C for 3 min and incubated overnight at hybridization temperature. Slides were then washed in 50% 0.5 \times formamide solution, washed in 0.5 \times sodium citrate, and blocked in ISH blocking solution (10% heat-inactivated sheep serum, 2% bovine serum albumen and 0.1% Triton-X100 in Tris-buffered saline). Following blocking, slides were incubated with anti-digoxigenin (1:500, Roche, IN, USA) antibody diluted in ISH block. Slides were then washed in Tris-buffered saline (pH 7.5, then pH 9.5) and incubated for 12–36 h in NBT/BCIP developing solution (1:50; Roche, IN, USA). Samples were visualized identically to immunohistochemical stains and processed using the same software.

2.5. Generation of hypothalamic neurospheres

For sphere generation, P1 pups were sacrificed by rapid decapitation and whole brains were removed. Brains were then placed ventral side up in a chilled neonatal mouse brain slicer (Zivic Instruments, PA, USA). A 2 mm coronal slice was collected beginning approximately at the mammillary body and extending rostrally, encompassing nearly the entire hypothalamus. Slices were moved into a dish of ice chilled PBS and a 1.25 mm³ tissue biopsy punch was collected at the most ventral end of the coronal slice. Punches from approximately 10 animals were pooled together in a solution of PBS containing 1 \times Anti-Anti solution (Thermo Fisher Scientific, MA, USA). Punches were rinsed 3 times with fresh PBS and dissociated mechanically via trituration with a P1000 pipette 30 times. Dissociated cells were centrifuged at 800 $\times g$ for 5 min, resuspended in Complete Media (CM, see formula below), and strained through a 0.22 μ m cell strainer.

2.6. Culture and passaging of neurospheres

Primary neurospheres were grown and passaged in Complete Media (CM) formulation composed of DMEM/F12 (Thermo Fisher Scientific, MA, USA) supplemented with 20 ng/mL human FGF basic (hFGFb) (R & D Systems, MN, USA), 20 ng/mL mouse EGF (mEGF) (R & D Systems, MN, USA), 2.92 μ g/mL L-Glutamine (Fisher Scientific, MA, USA), 2% B27 supplement (Thermo Fisher Scientific, MA, USA), and 1% Anti-Anti (Fungizone, 100 units/mL penicillin, and 100 μ g/mL streptomycin; Thermo Fisher Scientific, MA, USA). Initially, cells were plated in a T25 flask. After 3 days, cells were passaged via collection of suspended spheres. Flasks were gently rinsed to collect any loosely adherent spheres, selecting against tightly adherent glia and neurons. Cells were centrifuged as described above, resuspended in fresh CM, mechanically dissociated, and re-plated in a new T25. Three days following the first media change, spheres were expanded identically as described prior but into a T75 flask. Media was changed one final time and the fourth passage was plated for all experiments described. At this point, there were approximately 12 million cells present.

2.7. Cell plating for immunocytochemistry (ICC), RNA analysis, sphere size and MTT assays

To plate cells to visualize via ICC, glass coverslips were sterilized in 100% ethanol and placed in 12-well plates. Coverslips were coated with 0.01% Poly-L-Lysine (PLL) for 2 h prior to plating and rinsed twice with PBS. Spheres from the final passage were pelleted and resuspended mechanically in CM. Approximately 400,000–800,000 cells in 1 mL volume were plated in each well and allowed to grow for 72 h. For RNA analysis, 800,000 – 1,000,000 cells were plated in 0.5 mL volume in each well of uncoated 12-well plates for 72 h. Cells were treated with 10 μ M N-[N-(3,5-Difluorophenacetyl)-L-alanyl]-S-phenylglycine t-butyl ester (DAPT) or DMSO at the time of plating to determine the effect of Notch signaling. To determine sphere size and number, neurospheres were cultured and treated as described for RNA analysis, but prior to harvesting, each well of the 12 well plate was imaged at 10 \times in 3 random areas of the well. For each culture, 9 wells of spheres were

imaged for each treatment group (DMSO or DAPT). Sphere number and diameter was measured in each field using NIH ImageJ software. Sphere diameter was divided into 3 bin sizes, 50–100 μm , 100–200 μm , and 200+ μm . The total number of spheres as well as the number in each bin was averaged for DMSO or DAPT treatment. Five individual cultures were quantified for the sphere size and number measurements, and statistical analysis was performed in Microsoft Excel via the Student's two-tailed *t*-test. To determine the number of viable cells following DMSO and DAPT treatment, neurospheres were cultured and treated as described for RNA analysis. To quantify actively metabolic cells, 3-(4,5-dimethylthiazol-2-yl)-2,5-diphenyltetrazolium bromide (MTT, 5 mg/mL in PBS; Sigma, MO, USA) was added to the CM of the sphere culture and incubated for 3 h at 37 °C. Neurospheres were then harvested by centrifugation at 21,000 $\times g$ and formazan crystals resulting from the MTT incorporation were dissolved in 0.04 N HCl/Isopropanol. Number of viable cells per well was determined by optical density (O.D.) of the cell lysate measured at A_{570} . Data for the MTT assay was expressed as O.D. fold change of DAPT treatment vs. DMSO. An average of 4 replicated wells was taken for each treatment group and the MTT assay was repeated in 3 separate neurosphere cultures. Statistical significance was determined in Microsoft Excel via the Student's two-tailed *t*-test with a level of significance of $p < 0.05$.

2.8. Quantitative reverse transcriptase PCR (q-RT-PCR)

RNA was isolated from cultured spheres via TRIzol extraction method. 0.5 μg of RNA was synthesized into cDNA using the ProtoScript M-MuLV First Strand cDNA synthesis kit (New England BioLabs, MA, USA). For each culture, a no enzyme sample was included as a negative control. For q-RT-PCR analysis, 100 ng of cDNA was amplified using gene-specific primers diluted in SYBR green enzyme mix (Bio-Rad Laboratories, CA, USA) on a Bio-Rad MyIQ real-time PCR machine. Data were analyzed via the double change in threshold cycle ($\Delta\Delta\text{CT}$) method as previously described (Goldberg et al., 2011). Genes amplified via RTPCR/q-RT-PCR are found in Table 1. Samples were normalized to levels of the control genes *Rpl7*

or *Ppia* and statistical significance was determined in Microsoft Excel via the Student's two-tailed *t*-test with a level of significance of $p < 0.05$.

2.9. Image quantification

For counts of TH-positive cells and cell death via TUNEL at E13.5, 3 equally spaced sections parasagittal to the midline spanning the hypothalamus were stained and positive cells were quantified via an independent observer blind to the genotypes of each animal. For OLIG2 cell counts at P0, 4 representative coronal sections were chosen through the rostrocaudal extent of the AVPV and the number of OLIG2-positive cells within the area corresponding with ER α signal were quantified via an independent observer. Sections were chosen beginning at Bregma 3.68 mm and extended roughly 200 μm rostrally at P0 or 350 μm rostrally at P35 to capture the entire AVPV. Two sections per slide for $n = 3$ –4 animals of each genotype were calculated and the data represents the average number of positive cells per section and the standard error of the mean. Statistical significance was determined via Microsoft Excel via the Student's two-tailed *t*-test and significance was determined with $p < 0.05$.

For TH differentiation quantification in cultures, fluorescent micrographs of each channel (e.g., blue) were converted to 8-bit TIFF images in Fiji (ImageJ version 1.51a). Converted images were analyzed in CellProfiler (version 2.1.1) using the following modules: IdentifyPrimaryObjects to identify DAPI-labeled cell nuclei; IdentifySecondaryObjects to quantify TH intensity of cell soma; and MeasureNeurons to quantify TH intensity of neurites. Single-cell data from all three modules were output as CSV files using the ExportToSpreadsheet module for downstream analysis. Ensemble values for both soma and neurite TH intensity were calculated for each biological replicate; plotted values represent the mean and standard error of the mean for $n = 3$ biological replicates. An unpaired Wilcoxon rank sum test was used for all two-sample comparisons. For all hypothesis testing, $p < 0.05$ was considered significant.

Table 1

List of primers used within this study.

Gene Name	Forward: 5' → 3'	Reverse: 5' → 3'
<i>Nkx2.1</i>	GGTAGTTCAAATGGGTTCCCAAGC	AGTTTCAGGGCCATGGAAGCATAG
<i>Pomc</i>	TGGCTCAATGTCTCTCCTG	CACATAAGCTGCATCGTTAAG
<i>Kiss1</i>	TGCTGCTTCTCCTCTGT	ACCCGCGATTCTTTTCC
<i>Gfap</i>	TGAATCGCTGGAGGAGGA	TGTGAGGTCTGGCTTGGC
<i>Lhx2</i>	GCCAAGGACTTGAAGCAGCT	GGTTGCGCTGAACTTGGCC
<i>Sox2</i>	GGAGAAAGAAGAGGAGAGAG	CTGGCGGAGAATAGTTGG
<i>Sox9</i>	AGCCGACTCCCCACATTCTCC	GAGATTGCCAGAGTGCTGCCCC
<i>Notch1</i>	TTCCATGATTGCTCTGCACTGG	CAGGATCAGTGGAGTTGTGCCATCATGCA
<i>Notch2</i>	TGCCAATACTCCACCTCTC	TCCACTGACACTGCTTCC
<i>Notch3</i>	GAAGACCCTTGCCACTCAG	CCACGGAGACAACGACAG
<i>Notch4</i>	GAGGACCTGGTTGAAGAATTGATC	TGCAGTTTTTCCCTTTTATCCC
<i>Dll1</i>	TAACCTCGTTCGAGACCTCAAGGG	TGGCACTTGGTGTACAGTTTGC
<i>Dll3</i>	TCTCCCTCGTCATTGAAACCTGGA	GTAGGAGAAGTGCAACTCCATGT
<i>Jag1</i>	TGTAGCCAGAAAGTGACTGGTTG	TGTAGCCAGAAAGTGACTGGTTG
<i>Jag2</i>	TGGACACGAAAGCGCAGGAAAG	ACTGGTTGTTGGCGCTCTCATC
<i>Hey1</i>	TCTTGCAATGACTGTGG	ATGATGCTCAGATAACGG
<i>Hes1</i>	AAATGACTGTGAAGCACC	TCATGCACTCGCTGAAGC
<i>Hes5</i>	CGCATCAACAGCAGCATAGAG	TGGAAAGTGGTAAAGCAGCTTC
<i>Mash1</i>	TGGACTTTGGAAGCAGGATGG	TGACGTCGTTGGCGAGAAACA
<i>Rpl7</i>	CGCACTGAGATTCGGATG	TTAATTGAAGCCTTGTGAGC
<i>Ppia</i>	CAAATGCTGGACCAACACAAACG	GTTCATGCCTTCTTTACCTTCCC
<i>mKi67</i>	CCAGGGATCTCAGCGCAATTACAG	GGATAGGACAGAGGGCCACATTC
<i>Olig2</i>	CTAATTCACATTGGGAAGGTTG	GGACGATGGGCGACTAGAC
<i>Nes</i>	AGCAGGGTCTACAGAGTCAG	GTCTGTATGTAGCCACTTCC
<i>Lhx2</i>	GCCAAGGACTTGAAGCAGCT	GGTTGCGCCTGAACCTTGGCC
<i>Bax</i>	TGAAGACAGGGGCTTTTGT	AATTCGCCGAGACACTCG
<i>Bcl2</i>	ATGCCTTTGTGGAACATATATGGC	GGTATGCACCCAGAGTGATGC

2.10. Assessment of puberty

Control and *Rbpj* cKO females were checked for signs of puberty as early as P20. Vaginal opening was checked daily and puberty designated as the first day the vaginal canal remained open. Data are represented as the mean day of vaginal opening and standard error of the mean with significance determined via the Student's *t*-test with $p < 0.05$.

2.11. Analysis of sex steroid hormone levels

Blood was collected from 8-week old female mice ($n = 6–12$) in diestrus via cardiac puncture. Samples were allowed to clot, then centrifuged at $3000 \times g$ for 10 min to separate serum. Serum was then stored at -80°C until hormone levels were measured via enzyme linked immunosorbent assay (ELISA). Serum estradiol was measured via absorbance at 450 nm in comparison to a generated standard curve using a commercially available ELISA kit (DRG-2693; NJ, USA). All assays were performed according to manufacturer's protocol and all samples were run in duplicate with all coefficients of variability less than 10%. Data are represented as mean serum estradiol and standard error of the mean and significance was determined via the Student's *t*-test with $p < 0.05$.

3. Results

3.1. Notch receptors are present in the anterior hypothalamus and presumptive anteroventral periventricular nucleus (AVPV)

To explore the development of the anterior hypothalamus and nuclei that arise from it, we first sought to understand the region morphologically. Immunohistochemistry was used at E13.5 to detect the presence of TH-positive neurons, a commonly used marker to identify the AVPV (Simerly et al., 1985). In agreement with literature, a collection of TH-positive neurons was noted both within the ARC and near the ventricular zone along the rostral periventricular area of the third ventricle (RP3V) that then seemed to cluster within the region of the forming AVPV (Fig. 1A). We next sought to determine if the cells in the anterior hypothalamus indeed arose from *Nkx2.1* expressing early progenitor cells similar to other regions of the ventral diencephalon (Nakamura et al., 2001). Utilizing a genetic labeling tool of the tdTomato red fluorescent protein, any cell which ever expressed *Nkx2.1* during its development was labeled. A collection of tdTomato-positive labeled *Nkx2.1* cells in areas previously described, namely the ARC and posterior lobe of the pituitary (Nakamura et al., 2001) was noted. Interestingly, *Nkx2.1* expression was also observed in the more rostral area of the hypothalamus that corresponds with the developing AVPV (Fig. 1B). Double-staining of 5-week coronal sections reveals good concordance between tdTomato expression along the ventricle and in the lateral parenchyma and expression of both TH expressing (Fig. 1C) and kisspeptin expressing (Fig. 1D) neurons. This would suggest that both of these neuronal subtypes found within the adult indeed arose from an early *Nkx2.1* expressing common progenitor population.

To determine if Notch receptors were present in the accompanying ventricular zone, in situ hybridization was performed. In the ARC, the receptors *Notch1* and *Notch2* lined the continuum of the third ventricle and played an important role in neurogenesis and development of that hypothalamic area (Aujla et al., 2013). Similarly, we noted robust *Notch1* (Fig. 1D) and *Notch2* (Fig. 1E) mRNA expression along the entire HVZ, extending rostral to the area accompanying the TH-positive region of the developing AVPV. These results suggested that Notch signaling may play a role in the development of the AVPV as well.

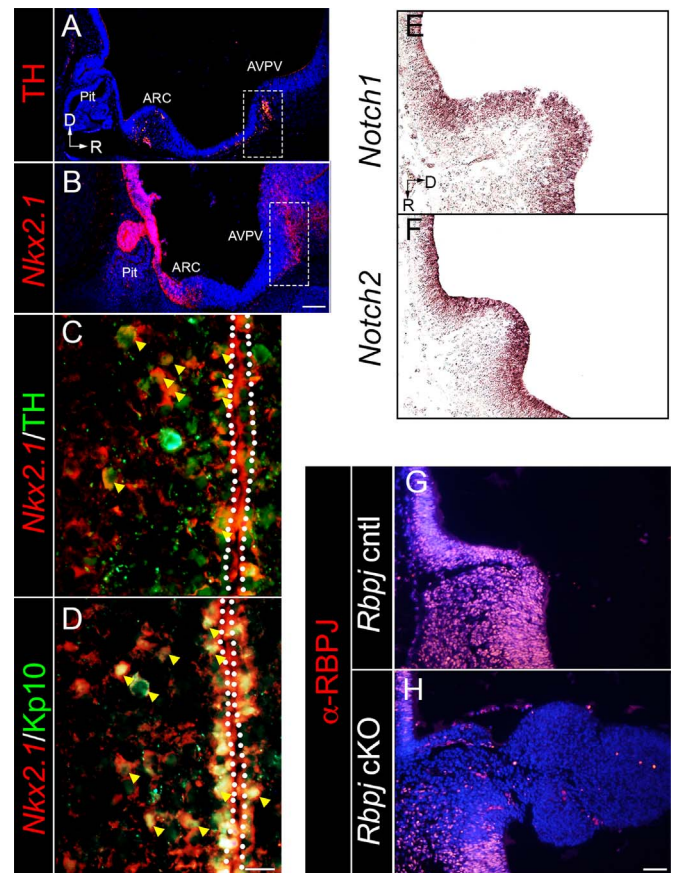


Fig. 1. Identification and characterization of the AVPV at E13.5. (A) The AVPV of the anterior hypothalamus was identified by expression of TH. Some TH neurons exist in the ARC and near the third ventricle (3V) in the periventricular area, and finally cluster in the presumptive AVPV (dashed line box). (B) *Nkx2.1* expression is marked by the tdTomato reporter. *Nkx2.1* expressing cells of the ventral diencephalon are found within the posterior lobe of the pituitary, ARC, and in a small area of the anterior hypothalamus (dashed line box). (C) *Nkx2.1* expression overlaps with TH-positive neurons of the AVPV, suggesting they develop from a common progenitor. (D) Kisspeptin (Kp10) expressing neurons of the AVPV also arise from an *Nkx2.1* expressing early lineage. White dots in (C) and (D) outline the area of the HVZ. (E) *Notch1* expression along the 3V in the developing AVPV. (F) *Notch2* expression along the 3V in the developing AVPV. (G) RBPJ protein expression is seen throughout the HVZ and underlying parenchyma in *Rbpj* control mice. (H) RBPJ expression is dramatically reduced when *Rbpj* is conditionally knocked out of *Nkx2.1* expressing progenitors (*Rbpj* cKO). Image magnification A, B = $100\times$, C, D = $400\times$, E–H = $200\times$. $n = 4$ (A), 3 (B–E). Pit = pituitary, ARC = arcuate nucleus. AVPV = anteroventral periventricular nucleus. Scale bar in (A) = $200\ \mu\text{m}$, (D) = $50\ \mu\text{m}$ (H) = $100\ \mu\text{m}$.

3.2. Conditional loss of *Rbpj* in the AVPV results in gross morphological differences and reduced active Notch signaling

In order to determine the function Notch signaling plays on development of this region, a mouse model of conditional deletion of *Rbpj* from *Nkx2.1* expressing cells was created. Within control animals (*Rbpj* cntl), RBPJ was readily detected throughout the extent of the HVZ and underlying presumptive AVPV at E13.5 (Fig. 1F). As expected, in the *Rbpj* conditional knock-out, in *Nkx2.1*-expressing progenitors (*Rbpj* cKO), RBPJ was selectively lost within the HVZ and the developing AVPV, which also appeared hyperplastic (Fig. 1G). In fact, the most noticeable phenotype in the *Rbpj* cKO was a morphological expansion of the underlying tissue of the presumptive AVPV (as well as the previously reported ARC), while other areas of the HVZ were unaffected (Fig. 2A, B). Following observation of the presence of Notch signaling components along the HVZ of the AVPV and given that active Notch signaling drives expression of multiple canonical downstream genes of the *Hes* family (Katoh and Katoh, 2007), we identified

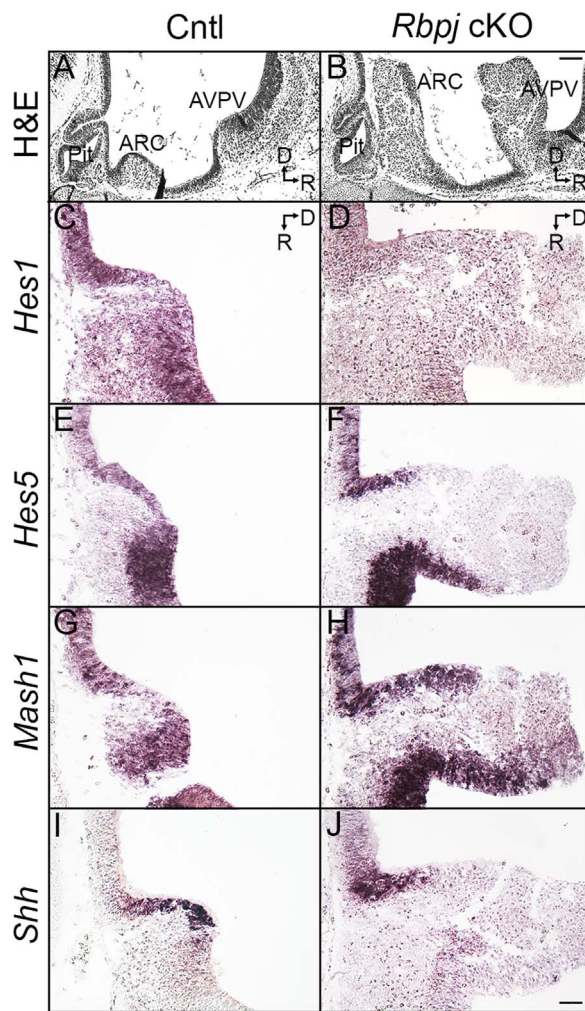


Fig. 2. Conditional loss of *Rbpj* results in AVPV hyperplasia and a reduction in Notch downstream targets at E13.5. (A) H&E of the developing ventral diencephalon in control and cKO (B) showing clear tissue expansion in both the ARC as well as the AVPV. (C) *Hes1* expression lines the HVZ in the AVPV in control mice. (D) *Hes1* expression is strikingly absent throughout the entire AVPV when *Rbpj* is lost. (E) *Hes5* is more robustly expressed in the HVZ in control mice and (F) is only absent in the more rostradorsal area of the AVPV corresponding with tissue expansion. (G) The proneural gene *Mash1* is modestly expressed through the HVZ in control mice. (H) In *Rbpj* cKO mice, *Mash1* expression is maintained but not increased as was observed in the ARC (Aujla et al., 2013). Expression is absent similarly in the most rostradorsal area of the AVPV. (I) *Shh* is present in the very caudal area of the AVPV in control mice. (J) *Shh* is maintained in the exact area of the AVPV in *Rbpj* cKO mice despite disruption in Notch targets. $n = 3-4$. Image magnification A,B = 100 \times , C-J = 200 \times . Pit = pituitary, ARC = arcuate nucleus, AVPV = anteroventral periventricular nucleus. Scale bar in (A) = 100 μ m and (J) = 50 μ m.

which *Hes* factors were present and affected by deletion of *Rbpj*. Weak expression of *Hes1* along the developing HVZ in control mice (Fig. 2C) was noted, while in *Rbpj* cKO mice *Hes1* was not detectable above background (Fig. 2D). However, expression of *Hes5* followed a different pattern: in control mice, *Hes5* was robustly expressed along the entire HVZ (Fig. 2E) but was notably absent only in the more dorsorostral area of the AVPV corresponding with the morphological tissue expansion in *Rbpj* cKO mice (Fig. 2F). This finding is especially interesting given that *Hes5* expression is maintained within the ARC of *Rbpj* cKO mice (Aujla et al., 2013). Finally, *Mash1*, a well-described proneural factor inhibited by the Notch targets *Hes1* and *Hes5*, within the AVPV was examined. *Mash1* expression was apparent throughout the HVZ (Fig. 2G) and interestingly, a corresponding increase in the AVPV of *Rbpj* cKO mice (Fig. 2H) was not observed. Dopaminergic neurons are the first detected neurons in the AVPV, and it is

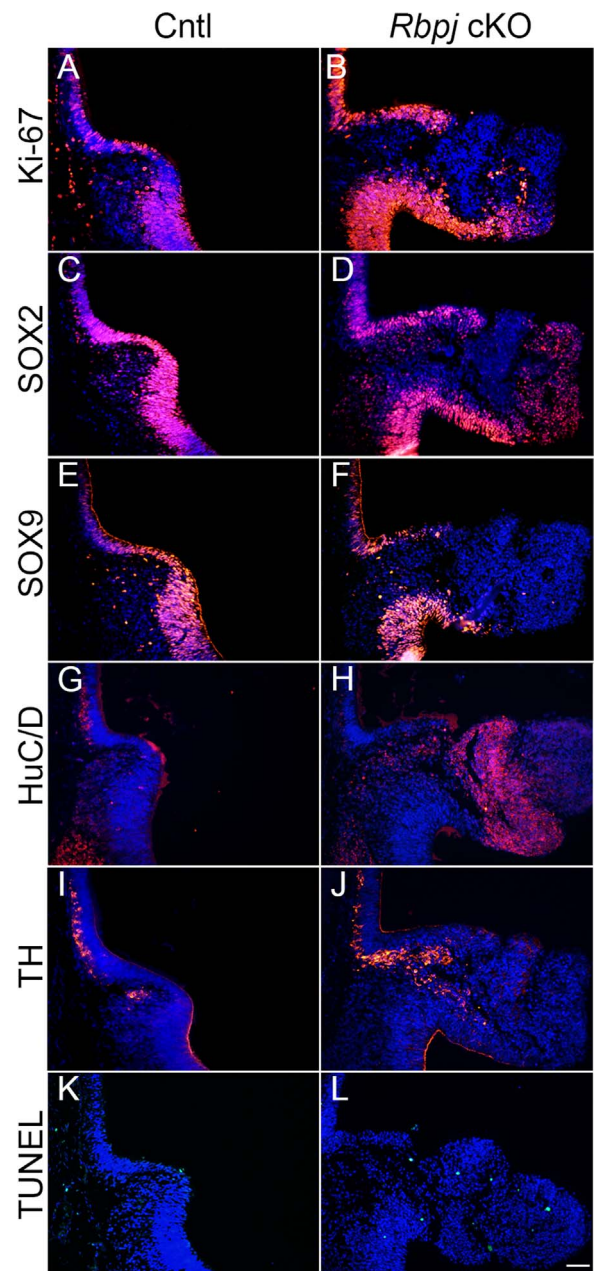


Fig. 3. Alterations to Notch signaling promote neurogenesis at E13.5. (A) Proliferation, as marked by Ki-67, is modest in control mice throughout the HVZ. (B) *Rbpj* cKO mice show increased proliferation through some of the HVZ with an abrupt loss corresponding with loss of *Hes5* expression (Fig. 2). (C) SOX2 expression appears to be similar to SOX9 expression throughout the HVZ in control animals. (D) SOX2 expression is mostly maintained with the loss of *Rbpj*, though cells appear to be less densely packed. (E) SOX9 positive progenitors are found throughout the HVZ in control mice. (F) Loss of *Rbpj* appears to result in a regional reduction in SOX9 intermediate neuronal progenitors. (G) Neurogenesis as marked by expression of HuC/D is somewhat modest by E13.5 in control mice. (H) Many more cells are positive for HuC/D in *Rbpj* cKO mice, specifically in the area ventral to SOX2 expression as observed in (D). (I) TH-positive neurons are present throughout both the periventricular area and AVPV in control animals. (J) Significantly more TH neurons, mainly in the AVPV, extending into the area of expansion are noted in *Rbpj* cKO mice. (K) Cellular apoptosis as marked by TUNEL stain is very low in control mice and restricted to the HVZ. (L) An increase of cell death is observed in *Rbpj* cKO mice, found both in the HVZ and underlying parenchyma. $n = 3-4$. Image magnification = 200 \times . Scale bar in L = 50 μ m.

hypothesized that the SHH pathway plays a critical role in their development (Hynes et al., 1995). With this knowledge, *Shh* expression in the AVPV was characterized. In control mice, *Shh* was restricted very specifically to the more caudal region of the AVPV, close to the area of

TH-positive neurons (Fig. 2I). Expression was maintained in *Rbpj* cKO mice in a very similar area despite a loss of *Hes1* and reduction in *Hes5*, suggesting that *Shh* is expressed independent of canonical Notch signaling in this region (Fig. 2J).

3.3. Loss of Notch signaling results in increased cellular proliferation and dopaminergic neurogenesis in the AVPV

Given the general role of Notch signaling in maintaining cells in a progenitor-like state and promoting proliferation, its function in the developing AVPV was examined. We began by exploring the dynamics of cells residing within the HVZ of the developing diencephalon. Using the antigen Ki-67 as a marker of cellular proliferation, a modest turnover throughout the HVZ of control mice (Fig. 3A) was noted. In *Rbpj* cKO mice, an increase in Ki-67 expression only in a specific region of the AVPV, corresponding very closely with *Hes5* expression (Fig. 3B) was noted. This finding may explain, in part, the expansion of the developing AVPV at this age. Given this observation, we then sought to identify what types of cells were found in overabundance in the AVPV. First, the expression of the progenitor cell markers from the Sry-related HMG box (SOX) family were characterized. SOX2, a progenitor cell marker identified as one of the four critical factors involved in stem cell maintenance (Takahashi and Yamanaka, 2006), is expressed in the developing neuroepithelium. Not surprisingly, SOX2 expression closely mimicked *Hes* family expression along the developing HVZ (Fig. 3C). Interestingly in *Rbpj* cKO mice, we did not notice a reduction or loss of SOX2-positive progenitors. Rather, cells were found mostly at the dorsal edge of the expansion of the AVPV as opposed to tightly clustered at the 3 V, potentially suggesting that either additional signaling pathways are playing a role in maintaining the progenitor pool of the AVPV or that Notch signaling is not involved in this process (Fig. 3D). Next, neuronal intermediates and neurogenesis were explored. In other regions of the brain such as the cerebellum, SOX9 expression serves as an intermediate precursor marker (Vong et al., 2015). Based on these findings, we hypothesized this may be the case in the hypothalamus as well and that loss of *Rbpj* may lead to reduced SOX9 expression due to premature neural differentiation. SOX9 expression was detected throughout the HVZ in control mice (Fig. 3E); however, little difference in SOX9 expression in *Rbpj* cKO mice (Fig. 3F) was noted. Notably, SOX9 was absent in the region absent of *Hes* signaling, suggesting that intermediate precursors are not maintained in areas devoid of active Notch signaling. We next hypothesized that many of the cells that were located in the area of expansion and not SOX2 positive had differentiated into neurons during this time point near the end of general neurogenesis. Using the general neuronal marker HuC/D, a very modest amount of differentiation though the HVZ and into the underlying parenchyma of the AVPV (Fig. 3G) was noted in control mice. However, a large increase in HuC/D expression throughout all of the underlying parenchyma of the AVPV in *Rbpj* cKO mice, complementing SOX2-positive cells present (Fig. 3H), was observed. The AVPV houses a population of dopaminergic TH-positive neurons as early as E13.5, so we next sought to determine if loss of *Rbpj* resulted in excess cells adopting a specific identity. In control mice, there were a number of TH neurons found within the tissue underlying the HVZ in the periventricular region up to the AVPV (13.6 ± 0.32 cells/section; $n = 3$ individual animals) (Fig. 3I). Interestingly, in *Rbpj* cKO mice, there were significantly more TH-positive neurons, specifically in the region of the AVPV extending into the area of tissue expansion (35.8 ± 1.07 cells/section; $n = 3$ individual animals) (Fig. 3J). It is important to note that there were many more observed HuC/D neurons within the AVPV, suggesting that other unexplored neuronal subtypes within this area may exist. Finally, given the excess proliferation and neurogenesis, we wanted to explore if an associated increase in cellular death would be observed, as it has been reported that apoptosis is a critical pathway in the development and sexual dimorphism observed within the mature AVPV (Forger et al., 2004). Upon assessing cellular death, little if any TUNEL-positive cells within the HVZ or underlying

parenchyma in control animals (Fig. 3K; 0.78 ± 0.20 positive cells/section; $n = 3$ individual animals) were noted. However, an increase in apoptotic cells in *Rbpj* cKO mice within the underlying parenchyma (Fig. 3L; 7.28 ± 1.16 cells/section; $n = 3$ individual animals) was observed. However, despite this increase, given the expansion of the region of interest, it is indeed possible that the process of apoptosis is not increased. Taken together, these data suggest a role for Notch signaling in restraining neuron numbers in the embryonic AVPV.

3.4. Loss of *Rbpj* results in a reduced ventricular zone and misplacement of differentiated cells in the parenchyma postnatally

While the presumptive AVPV appeared to be expanded at E13.5, it was important to examine how the region would appear morphologically into postnatal life and beyond. Hematoxylin and Eosin staining was performed on the day of birth (P0) through the periventricular region and into AVPV to assess gross morphology. Anatomical landmarks such as the optic chiasm, 3 V, and anterior commissure aided in identifying this region. In control mice, the HVZ was maintained throughout the periventricular area and the 3 V appeared to expand in the more rostral area just dorsal to the optic chiasm (Fig. 4A). Similar to what we previously published in the periventricular area of mice at 5 weeks of age, *Rbpj* cKO mice appeared normal in the more caudal periventricular area (Biehl and Raetzman, 2015) (data not shown). However, we consistently noted a region more rostral where the HVZ was strikingly reduced/absent in the developing AVPV (Fig. 4B). Given the abundance of TH differentiation at E13.5, the persistence of this phenomenon postnatally was explored. In control mice, TH-positive cells were organized very tightly on both sides of the lateral-dorsal aspect of the 3 V (Fig. 4C). Though still clearly present in *Rbpj* cKO mice, two interesting observations in regards to dopaminergic neurons were noted. First, while TH-positive cells were still readily detectable, they were not as clearly organized as control counterparts, likely due to the absence of a HVZ (Fig. 4D). Additionally, although there was an increase in TH-positive cells at E13.5, by P0 it would appear that expression is not strikingly different between each condition; rather, these cells are less tightly clustered near the presumptive HVZ and processes extended out further laterally, giving the appearance of a relative increase. These data would suggest an early neurogenic burst in *Rbpj* cKO mice that somewhat normalizes by birth. Given the region's role in regulation of reproductive function, another mature cellular subtype within the AVPV of interest are ER α -positive cells. One working hypothesis is these cells may be an early marker for kisspeptin neurons in the AVPV, since this specific subpopulation of kisspeptin neurons is not readily detectable until after P10 (Clarkson and Herbison, 2006; Kumar et al., 2015). In the early prepubertal window, roughly 30% of kisspeptin neurons express ER α and by adulthood over 70% of kisspeptin neurons also express ER α (Kumar et al., 2015). ER α -positive cells were readily detected in a very specific pattern lateral to the TH-positive neuron population previously described (Fig. 4E). Interestingly, in *Rbpj* cKO mice, positional differences between *Rbpj* control and cKO mice were noted; however, these differences were opposite of those observed in TH-positive cells. Instead of cells clustering closer to where the HVZ would have been in cKO mice, ER α cells appear to be present even further laterally than the organization observed in control mice (Fig. 4F). Finally, given the heterogeneity of cellular subtypes in each hypothalamic nucleus, we sought to characterize markers of other specific cell lineages at this age. Though a clear abundance in SOX2-positive cells in both control and *Rbpj* cKO mice embryonically (Fig. 3) were noted, we sought to determine if this observation was maintained into postnatal life and if there was a later wave of differentiation that may have been affected in *Rbpj* cKO mice. SOX2 expression was maintained at a very high level in both the HVZ and the parenchyma of the AVPV in control mice (Fig. 4G). Similar to observations at E13.5, SOX2 expression appeared to be maintained in the AVPV parenchyma in the *Rbpj* cKO model, but given the HVZ reduction, is less abundant along the ventricle

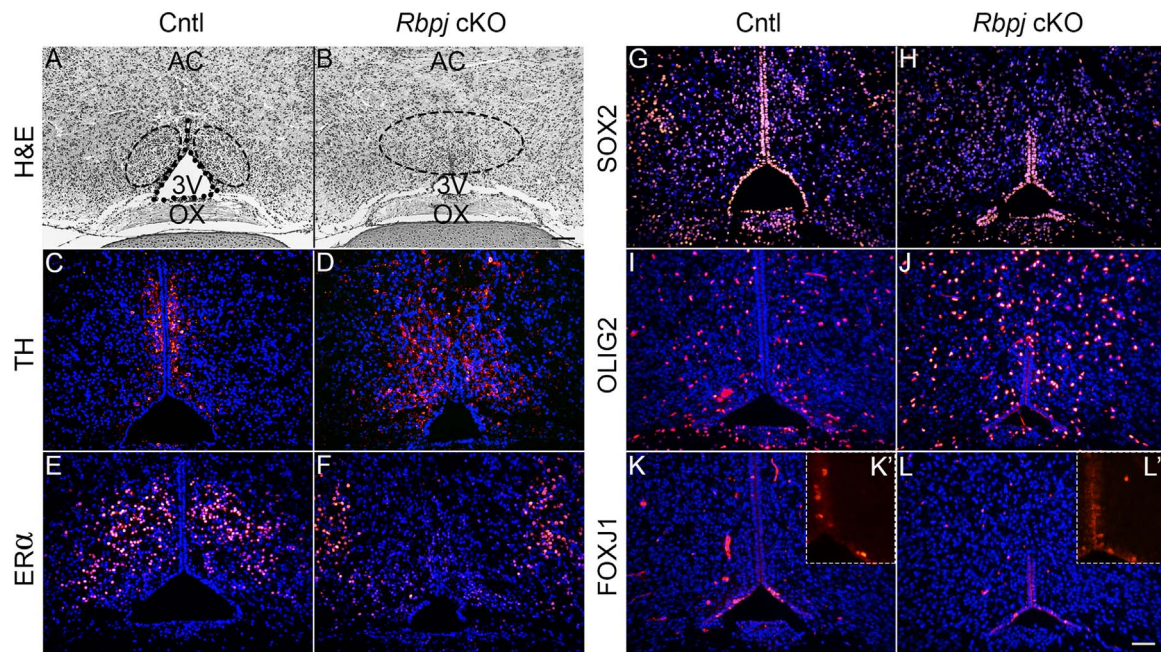


Fig. 4. Early loss of canonical Notch signaling results in failure to maintain the HVZ and increased oligodendrogenesis. (A) H & E of the AVPV at P0 reveals an open third ventricle (3V) and maintained HVZ. Anatomical landmarks such as the optic chiasm allowed for identification of the AVPV. (B) H & E of *Rbpj* cKO mice shows a dramatically reduced VZ and smaller 3V. (C) TH-positive neurons are organized along the dorsal area of the HVZ in the AVPV lining the 3V in control mice. (D) TH neurons are scattered throughout the parenchyma in *Rbpj* cKO mice, though they appear to somewhat cluster near where the HVZ would be maintained. (E) ERα-positive cells are expressed just lateral to the HVZ in the AVPV in control mice. (F) In *Rbpj* cKO mice, ERα positive cells appear disorganized and found far lateral to the presumptive VZ. (G) SOX2 expression is maintained in both the VZ and the parenchyma of the AVPV at P0 in control animals. (H) Similarly, SOX2 expression is found at a high level in the parenchyma and is present in cells of the remaining HVZ of the *Rbpj* cKO. (I) OLIG2, a marker of oligodendrocytic precursors, is found robustly scattered through the parenchyma of the AVPV in control females. (J) In *Rbpj* cKO females, OLIG2 is significantly increased, following the premature burst of neurogenesis at E13.5. (K, K') The ciliated ependymal marker FOXJ1 is expressed in multiple cells found within the HVZ in control mice. (L, L') FOXJ1 expression appears reduced corresponding to the reported failure to maintain HVZ progenitors in *Rbpj* cKO females. $n = 3-4$. Image magnification A,B = 100 \times , C-L = 200 \times . AVPV = anteroventral periventricular nucleus. OX = optic chiasm. AC = anterior commissure. Black dots line the area of the HVZ. Scale bar in (B) = 100 μ m, (L) 50 μ m.

(Fig. 4H). Another cellular lineage of the hypothalamus are oligodendrocytic precursor cells (OPCs), which give rise to glial cell subtypes of the hypothalamus and express a multitude of transcription factors during their development. One such early transcription factor of this lineage is the marker OLIG2 (Marsters et al., 2016a, 2016b). At P0, near the end of the major wave of gliogenesis, a number of OLIG2-positive cells scattered throughout the parenchyma of the AVPV in control females (Fig. 4I) were noted. In *Rbpj* cKO mice, statistically significantly more OLIG2-positive cells in the AVPV parenchyma were observed (40.5 ± 6.41 cells/section in control v. 63.8 ± 1.87 cells/section in cKO; $n = 3$ individual animals per condition) (Fig. 4J). These findings suggest that Notch signaling may restrain the process of gliogenesis along with neurogenesis. Finally, we sought to determine the role Notch signaling may be playing in development of one final lineage: ciliated ependymal cells. In control mice, a few cells found exclusively within the HVZ were positive for FOXJ1 (Fig. 4K). These cells were interspersed in the dorsal 3V along the ventricular wall (Fig. 4K'). While the HVZ is not entirely maintained in *Rbpj* cKO mice (Fig. 4B), the region most ventral, specifically the area which was maintained, had a number of FOXJ1 cells present (Fig. 4L), suggesting that specification of this lineage is unaltered. Indeed, FOXJ1 positive cells were found in the same region in *Rbpj* cKO mice as control counterparts (Fig. 4L'). Instead, failure to maintain the progenitor niche may contribute to why there appears to be a specific reduction of FOXJ1. Taken together, these data suggest that Notch signaling may be actively repressing differentiation of both neurons and oligodendrocytes during development.

3.5. Morphological and cellular abnormalities persist into the pubertal window in the AVPV

As discussed previously, one major role of the AVPV is control of onset of puberty and reproductive function (Hu et al., 2015). With this

knowledge, we wished to uncover if abnormalities would persist into the pubertal period in *Rbpj* cKO mice and to assess kisspeptin expression. Previously, we have shown that at P35 in the rostral area of the periventricular nucleus, TH neurons are abundant and near the 3V, whereas the kisspeptin population of neurons were absent in *Rbpj* cKO mice (Biehl and Raetzman, 2015). Further examination of the AVPV, however, a phenotype identical to P0 was apparent. At P35 in positionally matched tissue sections, TH-positive neurons were present in control (Fig. 5A) and *Rbpj* cKO mice (Fig. 5B), despite the abrupt absence of the HVZ in cKO mice. In the adult brain, a number of different types of glial cells can be found lining the 3V, including hypothalamic tanycytes, astrocytes, and other radial glia (Campbell et al., 2017). With this knowledge, we wanted to determine if hypothalamic glial cells were present and maintained in the absence of Notch signaling. To this end, the general glial marker GFAP was visualized at this same time point in the area where the HVZ was not maintained. In *Rbpj* control females, GFAP expression was highly concentrated in the HVZ with processes extending out into the underlying parenchyma (Fig. 5C). Additionally, we observed occasional astrocytic-like glia scattered throughout the parenchyma. In the absence of Notch signaling, notably in the area where the HVZ is not maintained, a profound disorganization in GFAP-positive clustering with some GFAP-positive cells scattered throughout the parenchyma (Fig. 5D) occurred. These findings suggest that, at this age, Notch signaling is necessary for structural maintenance of the HVZ. Finally, to determine if Notch signaling acted as a late fate selector of kisspeptin expressing neurons of the AVPV, kisspeptin expression was detected in control females along the 3V throughout the extent of the periventricular area and AVPV (Fig. 5E). Paralleling our observations in the ARC, virtually no kisspeptin-positive cell bodies and very few immunoreactive processes were detected throughout the entire AVPV (Fig. 5F, arrowheads) in *Rbpj* cKO mice.

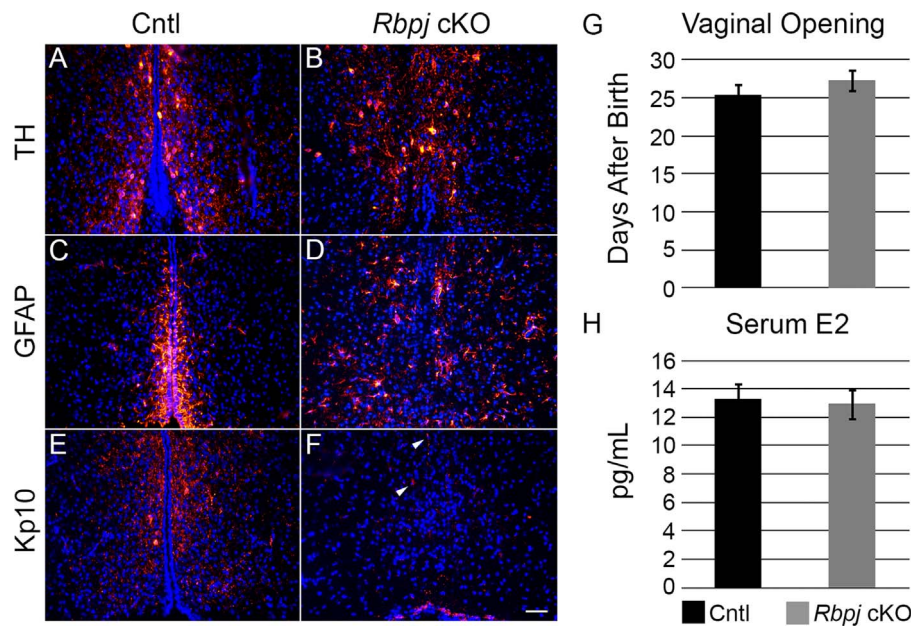


Fig. 5. *Rbpj* cKO females show reduced kisspeptin expression despite similar levels of circulating estradiol. (A) TH neurons of the AVPV are robust and found near the 3 V in control females. (B) Similar to observations at P0, TH neurons appear disorganized in *Rbpj* cKO females but located mostly near the presumptive HVZ. (C) GFAP-positive glia are mainly found densely packed along the 3 V with processes extending into the parenchyma. (D) GFAP appears reduced in *Rbpj* cKO females with some positive astrocytic cells scattered through the parenchyma. (E) Kisspeptin cell bodies and processes are detected throughout the AVPV near the HVZ. (F) A severe reduction in kisspeptin neurons are noted in *Rbpj* cKO mice, with occasional immunoreactive fibers detected through the continuum of the AVPV (arrowheads). (G) Day of vaginal opening to assess puberty is not different, suggesting estradiol is circulating at an appreciable level during the pubertal window. (H) Serum E2 as measured by ELISA shows no significant difference in estradiol at 8-weeks of age. $n = 4$ for histological analysis, 10–11 for vaginal opening, 6–12 for serum E2. Image magnification = 200 \times . Scale bar in (F) = 50 μ m. Error bars represent standard error of the mean.

3.6. *Rbpj* cKO females are not estrogenically compromised

One of the most potent activators of *Kiss1* expression in the AVPV is the presence of circulating estrogen (Cui et al., 2015). Previous work in our laboratory, as well as our current study, have provided evidence for the importance of Notch signaling in the development of kisspeptin neurons in both the ARC and AVPV (Biehl and Raetzman, 2015). *Rbpj* cKO mice showed a profound reproductive phenotype, where female mice were completely infertile and cycled irregularly (Biehl and Raetzman, 2015). Given these observations, we postulated that one explanation for the lack of observation of kisspeptin neurons in the AVPV and abnormal cyclicity was due, in part, to a lack of circulating estradiol. This may be due, in part, to underdevelopment of the ovaries and decreased production of circulating sex steroid. One early assessment of circulating serum estradiol is the day of vaginal opening (VO). Interestingly, *Rbpj* control and cKO mice had nearly identical days of VO (Fig. 5G). Additionally, circulating levels of estradiol in the serum of reproductively mature female *Rbpj* control and cKO mice was measured. At 8-weeks of age, female mice in diestrus were chosen given the previously reported irregularity in cyclicity. We found that both *Rbpj* control and cKO females had indistinguishable levels of estradiol in their serum (Fig. 5H), suggesting that the observed severe reduction in kisspeptin neurons is not due to the lack of estrogen stimulated gene expression and it is likely due to a failure of these neurons to properly develop.

3.7. Chemical inhibition of Notch signaling in vitro promotes an astrocytic-to-oligodendritic fate and biases dopaminergic neurogenesis

One major limitation with the in vivo data is that uncovering a mechanistic understanding of how Notch is acting directly at the level of hypothalamic progenitors is difficult. To this end, we chose to adopt and optimize a previously described hypothalamic neurosphere assay (Desai et al., 2011). Neurospheres initially were plated as mechanically dissociated individual cells from a ventral HVZ punch and over the

course of 12 days in vitro, expanded and formed large, well-defined sphere-like structures (Fig. 6A). Neurospheres harvested on the twelfth day of growth were then characterized to ensure they had active Notch signaling components as well as progenitor-like markers. Consistent with observations in vivo, multiple Notch receptors and ligands were detected by RT-PCR, as well as a number of downstream Notch targets and progenitor markers (Fig. 6B). Additionally, these spheres expressed progenitor and tanyocyte markers such as *Sox2*, *Sox9*, *Lhx2*, and *Gfap* yet did not express mature markers such as *Pomc* or *Kiss1* (Fig. 6B). In order to assess if Notch was able to be chemically manipulated in vitro, plated spheres were subjected to 10 μ M DAPT for 72 h to explore the effects on Notch signaling. A highly significant reduction in *Hes1*, *Hes5*, and *Hey1* and a robust increase in the proneural target of *Hes* and *Hey* family members, *Mash1* in the presence of DAPT (Fig. 7A) occurred. These findings together suggest that the hypothalamic neurospheres were progenitor-like in character and were able to have Notch signaling robustly manipulated in vitro.

We next sought to determine the effects of acute Notch inhibition on cellular proliferation and fate decisions to determine and how well this culture system recapitulates the in vivo findings. First, the ability of Notch signaling to restrain cellular proliferation, as seen in vivo, was probed with the in vitro system. Acute inhibition of Notch signaling by DAPT treatment was sufficient to augment proliferation as marked by *mKi67* mRNA expression on the day of sphere collection by over 3-fold compared to vehicle treatment (Fig. 7B). Additionally, we sought to determine if Notch inhibition would promote early gliogenesis and/or neurogenesis. Again similar to our in vivo reports, neurospheres treated with the Notch chemical inhibitor also showed a dramatic increase in the OPC marker *Olig2* mRNA (Fig. 7B). Additionally, we noted a dramatic decrease in *Gfap* expression, notably in a gene isoform restricted to astroglia (Fig. 7B) (Kamphuis et al., 2012) perhaps suggesting a role for Notch signaling during glial fate decisions in vitro as well. However, when we explored regulation of another glial subtype by examining the tanyocytic marker *Lhx2* (Salvatierra et al., 2014), we noted no difference in expression with DAPT treatment. Furthermore, when we compared the neuronal precursor marker

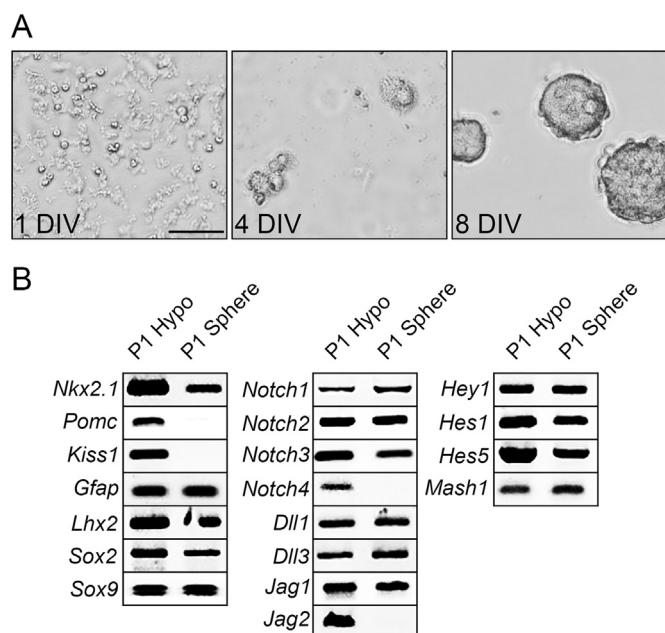


Fig. 6. Establishment and characterization of neurospheres. (A) Neurospheres were grown in complete media for 12 days in vitro prior to plating. Spheres progressed from growing as single cells to proliferating and forming spheroid-like structures each passage. (B) RTPCR of gene expression of harvested neurospheres following 12 days of culturing in vitro. Spheres still express several progenitor markers and Notch signaling components, yet lack differentiated markers. Scale bar in (A) = 200 μ m.

Nestin (*Nes*), we similarly observed no significant difference with 72 h DAPT treatment (Fig. 7B). Based on the induction in *mKi67* mRNA we observed in neurosphere cultures following Notch inhibition, we next sought to determine if this increase in proliferation resulted in more neurospheres or larger spheres. To address this, we quantified the total number of neurospheres in DMSO or DAPT treated cultures, as well as the number in 3 different size groups, 50–100 μ m, 100–200 μ m and 200+ μ m. We observed no differences in either the total number of neurospheres or the total number in any size group following Notch inhibition (Fig. 7C). Next, we assessed the viability of neurospheres treated with DMSO or DAPT by performing an MTT assay. Relative to the DMSO control, the DAPT treated neurospheres showed a significant reduction in viable cell number (Fig. 7D). This decreased viability following Notch inhibition prompted us to measure the levels of genes regulating cell death in the neurosphere cultures. We quantified mRNA from the pro-apoptotic gene *Bax* and the anti-apoptotic gene *Bcl2* in neurospheres treated with DMSO or DAPT. While we observed no change in *Bax* mRNA levels, *Bcl2* was significantly decreased following DAPT treatment (Fig. 7E). These data indicate that cell proliferation due to Notch inhibition in neurosphere cultures does not result in greater number of cells, possibly due to the initiation of apoptotic mechanisms.

Given that no bias in neuronal precursor fate after 72 h DAPT treatment, as marked by *Nes* gene expression, was observed, cultures were extended an additional 72 h in the presence of DAPT and the effects on dopaminergic neuronal fate decisions were determined. Vehicle treated neurospheres plated on coverslips expressed modest levels of TH observed both in the cell soma and short neurite extensions (Fig. 8A, C). After prolonged inhibition with DAPT, a distinct change in cell morphology occurred, as plated spheres began to take on a more neuronal appearance (Fig. 8B). Upon quantification, in both the cell soma and within the neurite extensions, there was about double the TH immunofluorescent intensity (Fig. 8C). Additionally, neurons had neurite extensions that were slightly, but statistically significantly, longer. Overall, these data demonstrate remarkable similarities between hypothalamic *Rbpj* cKO and DAPT

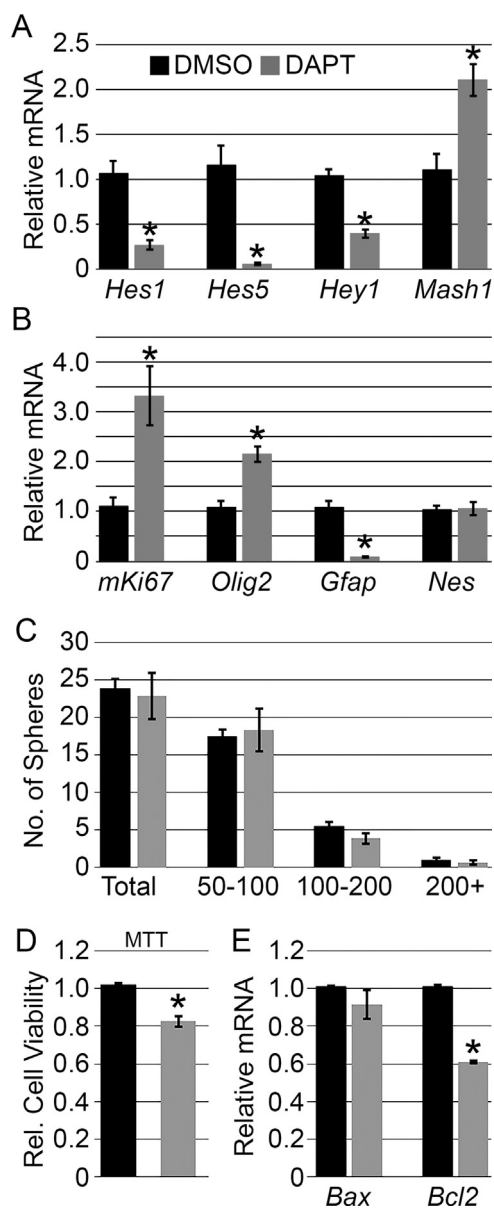


Fig. 7. Acute inhibition of Notch signaling in vitro promotes cell proliferation and oligodendrogenesis, but initiates cell death machinery. (A) 72 h inhibition of Notch signaling significantly reduces canonical downstream *Hes* and *Hey* targets, and promotes the proneural gene *Mash1*. (B) Notch inhibition increases cellular proliferation, as well as induces *Olig2* (early oligodendrocyte) expression and reduces *Gfap* (astroglia) expression. (C) Inhibition of Notch does not affect the total number of neurospheres or the size of spheres in vitro. Spheres are sorted into size groups of 50–100 μ m, 100–200 μ m or 200+ μ m. (D) MTT assay shows a significant decrease in cell viability of neurospheres treated with DAPT. (E) Anti-apoptotic gene *Bcl2* is down-regulated by Notch inhibition whereas the pro-apoptotic gene *Bax* is not affected. Data presented are average of combined wells from a single experiment. $n = 3–4$ wells/experiment repeated over 3–5 independent experiments. * = $p < 0.05$. Error bars represent standard error of the mean.

inhibition of Notch signaling in hypothalamic neurospheres, including proliferation, neural differentiation and oligodendrogenesis.

4. Discussion

This is one of the few studies of early development of the AVPV of the hypothalamus, specifically uncovering signaling pathways related to formation and cellular fate choices of this region. We report that Notch signaling is involved in the titration of cellular proliferation, as well as fate decisions including neurogenesis and gliogenesis in the

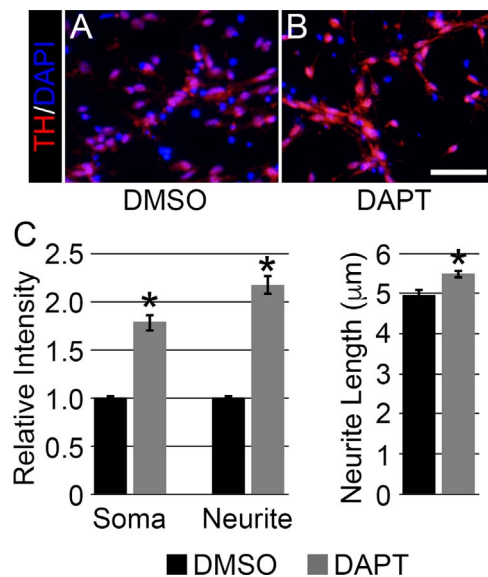


Fig. 8. Prolonged Notch inhibition in vitro promotes dopaminergic differentiation. Neurospheres plated on coverslips express modest levels of TH neuropeptide. (A) 144 h DAPT exposure modestly increases TH immunoreactivity and results in longer neurite extensions. (B) (C Left) Quantification of TH intensity (a.u.) in DMSO versus DAPT treatment in both cell soma and neurite extensions. (C Right) Neurite length is significantly longer in neurospheres treated 144 h with DAPT. Data represent $n = 3$ –4 cultures/experiment. Image magnification = 200 \times . Scale bar in B = 50 μ m.

embryonic period. Notch signaling is also necessary for preventing aberrant proliferation, neurogenesis, and OPC formation in vivo. However, it is not involved in progenitor cell maintenance in this area of the brain. Beyond the early developmental window, Notch signaling mediated by RBPJ-K is also required for proper formation of kisspeptin neurons of the AVPV, similar to what has been previously reported within the ARC (Biehl and Raetzman, 2015). The effects of Notch signaling reportedly appear to be acting on the progenitor population directly, as acute manipulation of Notch signaling in vitro appears to have very similar effects at the level of transcription on a population of pure progenitors.

One profound finding was that proliferation, as marked by Ki-67, was increased in vivo during embryonic hypothalamic development and in cultured postnatal progenitor cells with loss of Notch signaling. This observation suggests that a main function of Notch signaling is to restrain the cell cycle, thereby controlling the number of progeny created. This finding was somewhat surprising as Notch signaling is known to maintain the proliferating neural stem cell pool in vivo (reviewed in Yoon and Gaiano, 2005). Also, telencephalic neurospheres created from *Hes1*^{-/-}; *Hes5*^{-/-} mice were substantially reduced in size (Ohtsuka et al., 2001), again suggesting a role for Notch signaling in maintaining a proliferative progenitor state. These data indicate that the function of Notch signaling with regard to progenitor proliferation may be context specific and that the hypothalamus is somewhat unique. Another possibility is that Notch inhibition in hypothalamic development permits transition of stem cells into more highly proliferative intermediate progenitor cells, as observed in studies of *Rbpj* loss in embryonic telencephalon and neurospheres (Gao et al., 2009; Mizutani et al., 2007). Despite increased proliferation in the absence of Notch signaling in the hypothalamus, cell death may have been triggered in vivo and in vitro. Although the reason for this is unknown, it could be due to the inappropriately generated cells being unable to obtain optimal survival cues or to a direct regulation cell survival by Notch. Again, this regulation may be hypothalamic specific as Notch activation induces apoptosis in telencephalic neural progenitors (Yang et al., 2004).

Importantly, hypothalamic SOX2 progenitors can be maintained in the absence of *Rbpj*. Traditionally, Notch signaling promotes expres-

sion of genes of the *Hes* and *Hey* family (Jarriault et al., 1995). Transcription factors of this family are intimately associated with cellular proliferation and progenitor maintenance. However, in vivo loss of *Rbpj* and *Hes1*, and restriction of *Hes5*, resulted in an increase in cellular proliferation with no observable change in SOX2-positive progenitors in the HVZ (Figs. 2, 3). Given that *Rbpj* is genetically lost so early in development, it may be possible that other developmental signaling pathways may be compensating to support progenitor maintenance. Notch signaling has been shown to interact with and regulate numerous developmental pathway, including SHH and Wnt signaling (Giakoustidis et al., 2015). Each of these signaling pathways have also been reported to be potent regulators of the cell cycle, proliferation, and differentiation (Li et al., 2017; Szabo et al., 2009). Additional studies with acute Notch inhibition may clarify the role of Notch signaling in hypothalamic progenitor maintenance.

In our current study, we further suggest that Notch signaling restrains neurogenesis within the AVPV. We found that at E13.5, conditional loss of *Rbpj* resulted in an increase in both general neurogenesis (as marked by HuC/D) as well as a significant increase in more mature TH-positive neurons within the AVPV. However, by the day of birth and 5 weeks of age, this phenotype is modest or absent, which may hint that Notch signaling simply titrates the development of these neurons. These findings are similar to observations made previously within the ARC insofar that Notch signaling titrated *Pomc* neurogenesis in a similar fashion (Aujla et al., 2013; Biehl and Raetzman, 2015). We also report that canonical Notch signaling is necessary for the development of kisspeptin neurons in the AVPV similar to in the ARC. One hypothesis is that they are not fated to develop from the early embryonic period, potentially at the expense of an expansion of only TH-expressing neurons found within the periventricular area and AVPV. Early in development, it may be that canonical Notch signaling may also be interacting with the FGF signaling pathway, potentially by balancing expression of *Fgf8* or *Fgf1* in the presumptive AVPV. Indeed it has been shown that hypomorphs of either of these genes result in significantly more kisspeptin neurons of the AVPV, resulting in profound effects on day of VO and estrus cyclicity (Tata et al., 2012). It has also been reported that by reproductive maturity, a large portion of kisspeptin expressing neurons co-express TH (Clarkson and Herbison, 2011). However, there are also several neurons of the AVPV that only express the TH enzyme. Interestingly, the conversion of L-DOPA to dopamine occurring in these neurons potentially inhibits GnRH release, suggesting that the balance of neurons expressing each of these factors is vital for reproductive development in function (Liu and Herbison, 2013). In *Rbpj* cKO mice, it still remains a possibility that kisspeptin expressing neurons develop and do not express the kisspeptin peptide (but still express TH) since circulating levels of estrogen are necessary for maximal peptide expression within the AVPV (Smith et al., 2005). This seems unlikely, however, since *Rbpj* cKO female mice show both normal day of VO as well as similar levels of circulating E2 at 8 weeks of age, suggesting that appreciable levels of circulating sex steroids are present throughout development. Functionally, kisspeptin neurons of the AVPV respond positively to circulating estrogens to promote the onset of puberty, whereas kisspeptin neurons of the ARC are inhibited by circulating sex steroid and are hypothesized to be a reproductive brake (Takase et al., 2009). Despite these major functional differences, it is interesting to note that the signaling pathways underlying their early development are not apparently different. These findings provide further credence in our claims of the importance of canonical Notch signaling on neurogenesis within the AVPV, including development of TH- and kisspeptin-positive neurons.

Hypothalamic neurosphere cultures can be a good model to study the role of Notch signaling in neurogenesis. Treatment of neurospheres with the chemical Notch inhibitor DAPT quickly induced the proneural gene *Mash1*. Given the intimate relationship between *Mash1* expression and neurogenesis, especially within other regions of the hypothalamus,

lamus (McNay et al., 2006), we expected development of cultured neurospheres to begin to adopt a more neuronal-like phenotype. Interestingly, when we inhibited Notch signaling chemically for 6 days in vitro, a clear increase in TH expression occurred. This observation suggests that inhibiting Notch signaling for an extended period of time can indeed promote dopaminergic differentiation. It would be interesting to determine if stimulation of other signaling pathways, such as the addition of soluble SHH or manipulation of members of the bone morphogen protein (BMP) family, would exaggerate our findings (Hynes et al., 1995). In fact, it has been reported that at least SHH is sufficient to drive undifferentiated human embryonic stem (hES) cells towards a hypothalamic and neuronal identity in vitro (Wang et al., 2014). These cells can also be then further manipulated into functional dopaminergic neurons, presumably similar to those found within the AVPV. While these studies do successfully generate neurons of the hypothalamus, it is important to note that this process is very time and labor intensive, and may be more efficient in the context of a primary progenitor context similar to that discussed above.

Towards the end of the gliogenic window in *Rbpk* cKO mice, there was an increase in OLIG2-positive cells found within the parenchyma of the AVPV, where gliogenic progenitors are known to be located (Marsters et al., 2016a, 2016b). This suggests that in vivo, Notch signaling is not only necessary for titration of cellular proliferation and neurogenesis, but gliogenesis as well. Acutely inhibiting Notch signaling in hypothalamic neurospheres was also sufficient to induce *Olig2* mRNA expression and with a concomitant significantly reduced *Gfap* expression in an isoform directed at astrocytes, suggesting yet another fate switch. It is important to note, that *Gfap* is expressed in a large number of glial subtypes of the brain and, given the many isoforms of the *Gfap* gene, the region of the gene amplified can be telling in the cell population explored (Kamphuis et al., 2012) and given that our primer set used was directed at astrocytes, our findings can be amended to suggest Notch signaling is, in fact, playing more of a role in formation of OPCs and away from an astrocytic fate at this time period. Curiously, it has been reported that the Notch regulated proneural factor *Mash1/Ascl1* represses OPC formation in vivo (Marsters et al., 2016a, 2016b). However, in the context of hypothalamic neurospheres cultured beginning the day after birth, we report both increased in *Mash1* and *Olig2* expression with acute DAPT treatment. One explanation for this potential discrepancy may be that genetic ablation is permanent from an early stage, whereas acute inhibition is more temporally controlled suggesting that *Mash1/Ascl1* may also act at multiple stages of differentiation. Additionally, cultured progenitors may be more tanyctic in nature as opposed to early progenitors and thus the mode of regulation of *Mash1* may be slightly different within this context. Nevertheless, Notch signaling, namely its regulation of *Mash1*, appears to play a critical role in glial development and differentiation, perhaps acting as both an early and late fate selector of glial lineages of the CNS.

Other cellular subtypes explored within the AVPV were ciliated ependymal cells and specialized hypothalamic tanycytes. In *Rbpk* cKO mice, we noted a stark absence of the HVZ within the AVPV, likely resulting in decreased ependymal and tanycyte cell specification. Upon maturation, both of these cellular subtypes express the protein GFAP within the HVZ (Campbell et al., 2017). By 5 weeks of age, while GFAP was clearly still present in the *Rbpk* cKO, it was clearly disorganized throughout the parenchyma. While interpretation of these data are challenging owing to the fact that GFAP is expressed in so many subtypes within the hypothalamus (Kamphuis et al., 2012), it did provide us with evidence of the possibility that cells found within the HVZ may still be present even if the HVZ is not maintained. A more specific ependymal marker, FOXJ1, is commonly used to mark this cell type in the HVZ (Morimoto et al., 2010); however, it is postulated that active Notch represses FOXJ1 expression (Marcet et al., 2011). While we noted a potential reduction in FOXJ1 at P0, it is unclear in this model if Notch signaling is affecting HVZ maintenance or tanycyte and ependymal specification.

Overall, this study demonstrates the importance of Notch signaling in development of the AVPV. Seeing as many of our findings in vitro very closely parallel what we have previously reported in vivo (Aujla et al., 2013) as well as in vivo findings of our current study, we believe to have developed a new model to uncover the mechanism underlying neuronal differentiation and Notch signaling by further optimizing previously published assays for use with mouse models (Desai et al., 2016; Wang et al., 2014). The strength of the neurosphere model will allow for scanning of a much larger subset of genes in different contexts in order to more mechanistically understand fate choices on the developing hypothalamus.

Acknowledgements

We thank Changqing Zhou (Flaws Laboratory, University of Illinois at Urbana-Champaign) for technical support to generate serum hormone levels and perform ELISA experiments described above. This research was funded by National Institutes of Health R01 DK076647 (LTR), F30 DK105760 (MJB) and T32 ES007326 (MJB).

References

- Altman, J., Bayer, S.A., 1978. Development of the diencephalon in the rat II. correlation of the embryonic development of the hypothalamus with the time of origin of its neurons. *Com. Neurol.* 182, 973–993. <http://dx.doi.org/10.1002/cne.901880309>.
- Alvarez-Bolado, G., Paul, F.A., Blaess, S., 2012. Sonic hedgehog lineage in the mouse hypothalamus: from progenitor domains to hypothalamic regions. *Neural Dev.* 7, 4. <http://dx.doi.org/10.1186/1749-8104-7-4>.
- Aujla, P.K., Bogdanovic, V., Naratadam, G.T., Raetzman, L.T., 2015. Persistent expression of activated notch in the developing hypothalamus affects survival of pituitary progenitors and alters pituitary structure. *Dev. Dyn.* 244, 921–934. <http://dx.doi.org/10.1002/dvdy.24283>.
- Aujla, P.K., Naratadam, G.T., Xu, L., Raetzman, L.T., 2013. Notch/Rbpj signaling regulates progenitor maintenance and differentiation of hypothalamic arcuate neurons. *Development* 140, 3511–3521. <http://dx.doi.org/10.1242/dev.098681>.
- Biehl, M.J., Raetzman, L.T., 2015. Rbpj- κ mediated Notch signaling plays a critical role in development of hypothalamic Kisspeptin neurons. *Dev. Biol.* 406, 235–246. <http://dx.doi.org/10.1016/j.ydbio.2015.08.016>.
- Bodo, C., Kudwa, A.E., Rissman, E.F., 2006. Both estrogen receptor- α and - β are required for sexual differentiation of the anteroventral periventricular area in mice. *Endocrinology* 147, 415–420. <http://dx.doi.org/10.1210/en.2005-0834>.
- Campbell, J.N., Macosko, E.Z., Fenselau, H., Pers, T.H., Lyubetskaya, A., Tenen, D., Goldman, M., Verstegen, A.M.J., Resch, J.M., McCarroll, S.A., Rosen, E.D., Lowell, B.B., Tsai, L.T., 2017. A molecular census of arcuate hypothalamus and median eminence cell types. *Nat. Neurosci.* 20. <http://dx.doi.org/10.1038/nn.4495>.
- Casasola, S., Fode, C., Guillemot, F., 1999. *Mash1* regulates neurogenesis in the ventral telencephalon. *Development* 126, 525–534.
- Chakraborty, T.R., Rajendren, G., Gore, A.C., 2005. Expression of estrogen receptor {alpha} in the anteroventral periventricular nucleus of hypogonadal mice. *Exp. Biol. Med.* 230, 49–56.
- Chapouton, P., Webb, K.J., Stigloher, C., Alunni, A., Adolf, B., Hesl, B., Topp, S., Kremmer, E., Bally-Cuif, L., 2011. Expression of Hair/Enhancer of split genes in neural progenitors and neurogenesis domains of the adult zebrafish brain. *J. Comp. Neurol.* 519, 1748–1769. <http://dx.doi.org/10.1002/cne.22599>.
- Clarkson, J., Herbison, A.E., 2011. Dual phenotype kisspeptin-dopamine neurones of the rostral periventricular area of the third ventricle project to gonadotrophin-releasing hormone neurones. *J. Neuroendocrinol.* 23, 293–301. <http://dx.doi.org/10.1111/j.1365-2826.2011.02107.x>.
- Clarkson, J., Herbison, A.E., 2006. Postnatal development of kisspeptin neurons in mouse hypothalamus: sexual dimorphism and projections to gonadotropin-releasing hormone neurons. *Endocrinology* 147, 5817–5825. <http://dx.doi.org/10.1210/en.2006-0787>.
- Cui, P., Yang, C., Zhang, K., Gao, X., Luo, L., Tian, Y., Song, M., Liu, Y., Zhang, Y., Li, Y., Zhang, X., Su, S., Fang, F., Ding, J., 2015. Effect of estrogen on the expression of GnRH and kisspeptin in the hypothalamus of rats during puberty. *Theriogenology* 84, 1556–1564. <http://dx.doi.org/10.1016/j.theriogenology.2015.08.004>.
- de la Pompa, J.L., Wakeham, A., Correia, K.M., Samper, E., Brown, S., Aguilera, R.J., Nakano, T., Honjo, T., Mak, T.W., Rossant, J., Conlon, R., 1997. Conservation of the Notch signalling pathway in mammalian neurogenesis. *Development* 124, 1139–1148.
- De los Angeles García, M., Millán, C., Balmaceda-Aguilera, C., Castro, T., Pastor, P., Montecinos, H., Reinicke, K., Zúñiga, F., Vera, J.C., Oñate, S.A., Nualart, F., 2003. Hypothalamic ependymal-glial cells express the glucose transporter GLUT2, a protein involved in glucose sensing. *J. Neurochem.* 86, 709–724. <http://dx.doi.org/10.1046/j.1471-4159.2003.01892.x>.
- Desai, M., Han, G., Ross, M.G., 2016. Programmed hyperphagia in offspring of obese dams: altered expression of hypothalamic nutrient sensors, neurogenic factors and epigenetic modulators. *Appetite* 99, 193–199. <http://dx.doi.org/10.1016/j.appet.2016.01.023>.

- Desai, M., Li, T., Ross, M.G., 2011. Hypothalamic neurosphere progenitor cells in low birth-weight rat newborns: neurotrophic effects of leptin and insulin. *Brain Res.* 1378, 29–42. <http://dx.doi.org/10.1016/j.brainres.2010.12.080>.
- Duncan, R.N., Xie, Y., McPherson, A.D., Taibi, A.V., Bonkowski, J.L., Douglass, A.D., Dorsky, R.I., 2015. Hypothalamic radial glia function as self-renewing neural progenitors in the absence of Wnt/ss-catenin signaling. *Dev. Dev.*, 126813. <http://dx.doi.org/10.1242/dev.126813>.
- Ferran, J.L., Puellas, L., Rubenstein, J.L.R., 2015. Molecular codes defining rostrocaudal domains in the embryonic mouse hypothalamus. *Front. Neuroanat.* 9, 46. <http://dx.doi.org/10.3389/fnana.2015.00046>.
- Forger, N.G., Rosen, G.J., Waters, E.M., Jacob, D., Simerly, R.B., de Vries, G.J., 2004. Deletion of Bax eliminates sex differences in the mouse forebrain. *Proc. Natl. Acad. Sci. USA* 101, 13666–13671. <http://dx.doi.org/10.1073/pnas.040464101>.
- Gao, F., Zhang, Q., Zheng, M.-H., Liu, H.-L., Hu, Y.-Y., Zhang, P., Zhang, Z.-P., Qin, H.-Y., Feng, L., Wang, L., Han, H., Ju, G., 2009. Transcription factor RBP-J-mediated signaling represses the differentiation of neural stem cells into intermediate neural progenitors. *Mol. Cell. Neurosci.* 40, 442–450. <http://dx.doi.org/10.1016/j.mcn.2008.12.008>.
- García, M.A., Millán, C., Balmaceda-Aguilera, C., Castro, T., Pastor, P., Montecinos, H., Reinicke, K., Zúñiga, F., Vera, J.C., Oñate, S.A., Nualart, F., 2003. Hypothalamic ependymal-glial cells express the glucose transporter GLUT2, a protein involved in glucose sensing. *J. Neurochem.* 86, 709–724.
- Giakoustidis, A., Giakoustidis, D., Mudan, S., Sklavos, A., Williams, R., 2015. Molecular signalling in hepatocellular carcinoma: role of and crosstalk among WNT/β-catenin, Sonic Hedgehog, Notch and Dickkopf-1. *Can. J. Gastroenterol. Hepatol.* 29, 209–217.
- Goldberg, L.B., Aujla, P.K., Raetzman, L.T., 2011. Persistent expression of activated Notch inhibits corticosterone and melanocyte differentiation and results in dysfunction of the HPA axis. *Dev. Biol.* 358, 23–32. <http://dx.doi.org/10.1016/j.ydbio.2011.07.004>.
- Han, S.K., Gottsch, M.L., Lee, K.J., Popa, S.M., Smith, J.T., Jakawich, S.K., Clifton, D.K., Steiner, R.A., Herbison, A.E., 2005. Activation of gonadotropin-releasing hormone neurons by kisspeptin as a neuroendocrine switch for the onset of puberty. *J. Neurosci.* 25, 11349–11356. <http://dx.doi.org/10.1523/JNEUROSCI.3328-05.2005>.
- Horvath, T.L., Sarman, B., García-Cáceres, C., Enriori, P.J., Sotonyi, P., Shanabrough, M., Borok, E., Argente, J., Chown, J.A., Perez-Tilve, D., Pfluger, P.T., Brönneke, H.S., Levin, B.E., Diano, S., Cowley, M.A., Tschöp, M.H., 2010. Synaptic input organization of the melanocortin system predicts diet-induced hypothalamic reactive gliosis and obesity. *Proc. Natl. Acad. Sci. USA* 107, 14875–14880. <http://dx.doi.org/10.1073/pnas.1004282107>.
- Hu, M.H., Li, X.F., McCausland, B., Li, S.Y., Gresham, R., Kinsey-Jones, J.S., Gardiner, J.V., Sam, A.H., Bloom, S.R., Poston, L., Lightman, S.L., Murphy, K.G., O'Byrne, K.T., 2015. Relative importance of the arcuate and anteroventral periventricular kisspeptin neurons in control of puberty and reproductive function in female rats. *Endocrinology* 156, 2619–2631. <http://dx.doi.org/10.1210/en.2014-1655>.
- Hynes, M., Porter, J.A., Chiang, C., Chang, D., Tessier-Lavigne, M., Beachy, P.A., Rosenthal, A., 1995. Induction of midbrain dopaminergic neurons by sonic hedgehog. *Neuron* 15, 35–44. [http://dx.doi.org/10.1016/0896-6273\(95\)90062-4](http://dx.doi.org/10.1016/0896-6273(95)90062-4).
- Jacquet, B.V., Salinas-Mondragon, R., Liang, H., Therit, B., Buie, J.D., Dykstra, M., Campbell, K., Ostrowski, L.E., Brody, S.L., Ghashghaei, H.T., 2009. FoxJ1-dependent gene expression is required for differentiation of radial glia into ependymal cells and a subset of astrocytes in the postnatal brain. *Development* 136, 4021–4031. <http://dx.doi.org/10.1242/dev.041129>.
- Jarriault, S., Brou, C., Logeat, F., Schroeter, E.H., Kopan, R., Israel, A., 1995. Signalling downstream of activated mammalian Notch. *Nature* 377, 355–358. <http://dx.doi.org/10.1038/377355a0>.
- Kamphuis, W., Mamber, C., Moeton, M., Kooijman, L., Sluijs, J.A., Jansen, A.H.P., Verveer, M., de Groot, L.R., Smith, V.D., Rangarajan, S., Rodriguez, J.J., Orre, M., Hol, E.M., 2012. GFAP isoforms in adult mouse brain with a focus on neurogenic astrocytes and reactive astrogliosis in mouse models of Alzheimer disease. *PLoS One* 7, e42823. <http://dx.doi.org/10.1371/journal.pone.0042823>.
- Katoh, M., Katoh, M., 2007. Integrative genomic analyses on HES/HEY family: notch-independent HES1, HES3 transcription in undifferentiated ES cells, and Notch-dependent HES1, HES5, HEY1, HEY2, HEYL transcription in fetal tissues, adult tissues, or cancer. *Int. J. Oncol.* 31, 461–466. (doi:17611704).
- Kumar, D., Candlish, M., Periasamy, V., Avcu, N., Mayer, C., Boehm, U., 2015. Specialized subpopulations of kisspeptin neurons communicate with GnRH neurons in female mice. *Endocrinology* 156, 32–38. <http://dx.doi.org/10.1210/en.2014-1671>.
- Kusakabe, T., Kawaguchi, A., Hoshi, N., Kawaguchi, R., Hoshi, S., Kimura, S., 2006. Thyroid-specific enhancer-binding protein/NKX2.1 is required for the maintenance of ordered architecture and function of the differentiated thyroid. *Mol. Endocrinol.* 20, 1796–1809. <http://dx.doi.org/10.1210/me.2005-0327>.
- Le Foll, C., Dunn-Meynell, A.A., Miziorko, H.M., Levin, B.E., 2014. Regulation of hypothalamic neuronal sensing and food intake by ketone bodies and fatty acids. *Diabetes* 63, 1259–1269. <http://dx.doi.org/10.2337/db13-1090>.
- Li, M., Dai, Y., Wang, L., Li, L., 2017. Astrocyte elevated gene-1 promotes the proliferation and invasion of breast cancer cells by activating the Wnt/β-catenin signaling pathway. *Oncol. Lett.* 13, 2385–2390. <http://dx.doi.org/10.3892/ol.2017.5695>.
- Liu, X., Herbison, A.E., 2013. Dopamine regulation of gonadotropin-releasing hormone neuron excitability in male and female mice. *Endocrinology* 154, 340–350. <http://dx.doi.org/10.1210/en.2012-1602>.
- Lu, J., Zhou, Y., Hu, T., Zhang, H., Shen, M., Cheng, P., Dai, W., Wang, F., Chen, K., Zhang, Y., Wang, C., Li, J., Zheng, Y., Yang, J., Zhu, R., Wang, J., Lu, W., Zhang, H., Wang, J., Xia, Y., De Assuncao, T.M., Jalan-Sakrikar, N., Huebert, R.C., Bin, Zhou, Guo, C., 2016. Notch signaling coordinates progenitor cell-mediated biliary regeneration following partial hepatectomy. *Sci. Rep.* 6, 22754. <http://dx.doi.org/10.1038/srep22754>.
- Madisen, L., Zwingman, T.A., Sunkin, S.M., Oh, S.W., Hatim, A., Gu, H., Ng, L.L., Palmiter, R.D., Hawrylycz, M.J., Allan, R., Lein, E.S., Zeng, H., 2010. A robust and high-throughput Cre Reporting and characterization. *Nat. Neurosci.* 13, 133–140. <http://dx.doi.org/10.1038/nn.2467>.
- Marcel, B., Chevalier, B., Coraux, C., Kodjabachian, L., Barbry, P., 2011. MicroRNA-based silencing of Delta/Notch signaling promotes multiple cilia formation. *Cell Cycle* 10, 2858–2864. <http://dx.doi.org/10.4161/cc.10.17.17011>.
- Marsters, C.M., Rosin, J.M., Thornton, H.F., Aslanpour, S., Klenin, N., Wilkinson, G., Schuurmans, C., Pittman, Q.J., Kurrasch, D.M., 2016a. Oligodendrocyte development in the embryonic tuberal hypothalamus and the influence of Ascl1. *Neural Dev.* 11, 20. <http://dx.doi.org/10.1186/s13064-016-0075-9>.
- Marsters, C.M., Rosin, J.M., Thornton, H.F., Aslanpour, S., Klenin, N., Wilkinson, G., Schuurmans, C., Pittman, Q.J., Kurrasch, D.M., 2016b. Oligodendrocyte development in the embryonic tuberal hypothalamus and the influence of Ascl1. *Neural Dev.* 11, 20. <http://dx.doi.org/10.1186/s13064-016-0075-9>.
- McNay, D.E.G., Pelling, M., Claxton, S., Guillemot, F., Ang, S.-L., 2006. Mash1 Is required for generic and subtype differentiation of hypothalamic neuroendocrine cells. *Mol. Endocrinol.* 20, 1623–1632. <http://dx.doi.org/10.1210/me.2005-0518>.
- Melcangi, R.C., Celotti, F., Ballabio, M., Castano, P., Poletti, A., Milani, S., Martini, L., 1988. Ontogenetic development of the 5 alpha-reductase in the rat brain: cerebral cortex, hypothalamus, purified myelin and isolated oligodendrocytes. *Brain Res. Dev.* 44, 181–188.
- Micevych, P., Sinchak, K., Mills, R.H., Tao, L., LaPolt, P., Lu, J.K.H., 2003. The luteinizing hormone surge is preceded by an estrogen-induced increase of hypothalamic progesterone in ovariectomized and adrenalectomized rats. *Neuroendocrinology* 78, 29–35. (doi:171703).
- Miller, S.A., Dykes, D.D., Polesky, H.F., 1988. A simple salting out procedure for extracting DNA from human nucleated cells. *Nucleic Acids Res.* 16, 1215. <http://dx.doi.org/10.1093/nar/16.3.1215>.
- Miranda-Angulo, A.L., Byerly, M.S., Mesa, J., Wang, H., Blackshaw, S., 2014. Rax regulates hypothalamic tanyocyte differentiation and barrier function in mice. *J. Comp. Neurol.* 522, 876–899. <http://dx.doi.org/10.1002/cne.23451>.
- Mizutani, K., Yoon, K., Dang, L., Tokunaga, A., Gaiano, N., 2007. Differential Notch signalling distinguishes neural stem cells from intermediate progenitors. *Nature* 449, 351–355. <http://dx.doi.org/10.1038/nature06090>.
- Morimoto, M., Liu, Z., Cheng, H.-T., Winters, N., Bader, D., Kopan, R., 2010. Canonical Notch signaling in the developing lung is required for determination of arterial smooth muscle cells and selection of Clara versus ciliated cell fate. *J. Cell Sci.* 123, 213–224. <http://dx.doi.org/10.1242/jcs.058669>.
- Nakamura, K., Kimura, S., Yamazaki, M., Kawaguchi, A., Inoue, K., Sakai, T., 2001. Immunohistochemical analyses of thyroid-specific enhancer-binding protein in the fetal and adult rat hypothalamic and pituitary glands. *Dev. Brain Res.* 130, 159–166. [http://dx.doi.org/10.1016/S0165-3806\(01\)00226-7](http://dx.doi.org/10.1016/S0165-3806(01)00226-7).
- Nery, S., Wichterle, H., Fishell, G., 2001. Sonic hedgehog contributes to oligodendrocyte specification in the mammalian forebrain. *Development* 128, 527–540.
- Ohtsuka, T., Sakamoto, M., Guillemot, F., Kageyama, R., 2001. Roles of the basic helix-loop-helix genes Hes1 and Hes5 in expansion of neural stem cells of the developing brain. *J. Biol. Chem.* 276, 30467–30474. <http://dx.doi.org/10.1074/jbc.M102420200>.
- Okigawa, S., Mizoguchi, T., Okano, M., Tanaka, H., Isoda, M., Jiang, Y.J., Suster, M., Higashijima, S. ichi, Kawakami, K., Itoh, M., 2014. Different combinations of Notch ligands and receptors regulate V2 interneuron progenitor proliferation and V2a/V2b cell fate determination. *Dev. Biol.* 391, 196–206. <http://dx.doi.org/10.1016/j.ydbio.2014.04.011>.
- Peng, C.-Y., Mukhopadhyay, A., Jarrett, J.C., Yoshikawa, K., Kessler, J.A., 2012. BMP receptor 1A regulates development of hypothalamic circuits critical for feeding behavior. *J. Neurosci.* 32, 17211–17224. <http://dx.doi.org/10.1523/JNEUROSCI.2484-12.2012>.
- Ramasamy, S.K., Lenka, N., 2010. Notch exhibits ligand bias and maneuvers stage-specific steering of neural differentiation in embryonic stem cells. *Mol. Cell. Biol.* 30, 1946–1957. <http://dx.doi.org/10.1128/MCB.01419-09>.
- Robins, S.C., Stewart, I., McNay, D.E., Taylor, V., Giachino, C., Goetz, M., Ninkovic, J., Briancon, N., Maratos-Flier, E., Flier, J.S., Kokoeva, M.V., Placzek, M., 2013. α-Tanyocytes of the adult hypothalamic third ventricle include distinct populations of FGF-responsive neural progenitors. *Nat. Commun.* 4, 2049. <http://dx.doi.org/10.1038/ncomms3049>.
- Salgado, M., Tarifeño-Saldivia, E., Ordenes, P., Millán, C., Yañez, M.J., Llanos, P., Villagra, M., Elizondo-Vega, R., Martínez, F., Nualart, F., Uribe, E., De Los Angeles García-Robles, M., 2014. Dynamic localization of glucokinase and its regulatory protein in hypothalamic tanyocytes. *PLoS One* 9. <http://dx.doi.org/10.1371/journal.pone.0094035>.
- Salvatierra, J., Lee, D.A., Zibetti, C., Duran-Moreno, M., Yoo, S., Newman, E.A., Wang, H., Bedont, J.L., de Melo, J., Miranda-Angulo, A.L., Gil-Perotin, S., García-Verdugo, J.M., Blackshaw, S., 2014. The LIM homeodomain factor Lhx2 is required for hypothalamic tanyocyte specification and differentiation. *J. Neurosci.* 34, 16809–16820. <http://dx.doi.org/10.1523/JNEUROSCI.1711-14.2014>.
- Simerly, R.B., Swanson, L.W., Gorski, R.A., 1985. The distribution of monoaminergic cells and fibers in a periventricular preoptic nucleus involved in the control of gonadotropin release: immunohistochemical evidence for a dopaminergic sexual dimorphism. *Brain Res.* 330, 55–64. [http://dx.doi.org/10.1016/0006-8993\(85\)90007-1](http://dx.doi.org/10.1016/0006-8993(85)90007-1).
- Smith, J.T., Cunningham, M.J., Rissman, E.F., Clifton, D.K., Steiner, R.A., 2005.

- Regulation of Kiss1 gene expression in the brain of the female mouse. *Endocrinology* 146, 3686–3692. <http://dx.doi.org/10.1210/en.2005-0488>.
- Szabo, N.-E., Zhao, T., Cankaya, M., Theil, T., Zhou, X., Alvarez-Bolado, G., 2009. Role of neuroepithelial sonic hedgehog in hypothalamic patterning. *J. Neurosci.* 29, 6989–7002. <http://dx.doi.org/10.1523/JNEUROSCI.1089-09.2009>.
- Takahashi, K., Yamanaka, S., 2006. Induction of pluripotent stem cells from mouse embryonic and adult fibroblast cultures by defined factors. *Cell* 126, 663–676. <http://dx.doi.org/10.1016/j.cell.2006.07.024>.
- Takase, K., Uenoyama, Y., Inoue, N., Matsui, H., Yamada, S., Shimizu, M., Homma, T., Tomikawa, J., Kanda, S., Matsumoto, H., Oka, Y., Tsukamura, H., Maeda, K.-I., 2009. Possible role of oestrogen in pubertal increase of Kiss1/Kisspeptin expression in discrete hypothalamic areas of female rats. *J. Neuroendocrinol.* 21, 527–537. <http://dx.doi.org/10.1111/j.1365-2826.2009.01868.x>.
- Tanigaki, K., Tsuji, M., Yamamoto, N., Han, H., Tsukada, J., Inoue, H., Kubo, M., Honjo, T., 2004. Regulation of alphabeta/gammadelta T cell lineage commitment and peripheral T cell responses by Notch/RBP-J signaling. *Immunity* 20, 611–622. [http://dx.doi.org/10.1016/S1074-7613\(04\)00109-8](http://dx.doi.org/10.1016/S1074-7613(04)00109-8).
- Tata, B.K., Chung, W.C.J., Brooks, L.R., Kavanaugh, S.I., Tsai, P.-S., 2012. Fibroblast growth factor signaling deficiencies impact female reproduction and Kisspeptin Neurons in Mice1. *Biol. Reprod.* 86, 119. <http://dx.doi.org/10.1095/biolreprod.111.095992>.
- Truett, G.E., Heeger, P., Mynatt, R.L., Truett, A.A., Walker, J.A., Warman, M.L., 2000. Preparation of PCR-quality mouse genomic DNA with hot sodium hydroxide and tris (HotSHOT). *Biotechniques* 29 (52), 54.
- Vong, K.I., Leung, C.K.Y., Behringer, R.R., Kwan, K.M., 2015. Sox9 is critical for suppression of neurogenesis but not initiation of gliogenesis in the cerebellum. *Mol. Brain* 8, 25. <http://dx.doi.org/10.1186/s13041-015-0115-0>.
- Walsh, R.J., Brawer, J.R., Lin, P.L., 1978. Early postnatal development of ependyma in the third ventricle of male and female rats. *Am. J. Anat.* 151, 377–407.
- Wang, L., Meece, K., Williams, D.J., Lo, K.A., Zimmer, M., Heinrich, G., Carli, J.M., Leduc, C.A., Sun, L., Zeltser, L.M., Freeby, M., Goland, R., Tsang, S.H., Wardlaw, S.L., Egli, D., Leibel, R.L., 2014. Differentiation of hypothalamic-like neurons from human pluripotent stem cells. *J. Clin. Investig.* 1, 1–13. <http://dx.doi.org/10.1172/JCI79220DS1>.
- Yang, X., Klein, R., Tian, X., Cheng, H.-T., Kopan, R., Shen, J., 2004. Notch activation induces apoptosis in neural progenitor cells through a p53-dependent pathway. *Dev. Biol.* 269, 81–94. <http://dx.doi.org/10.1016/j.ydbio.2004.01.014>.
- Yee, C.L., Wang, Y., Anderson, S., Ekker, M., Rubenstein, J.L.R., 2009. Arcuate nucleus expression of NKX2.1 and DLX and lineages expressing these transcription factors in neuropeptide Y(+), proopiomelanocortin(+), and tyrosine hydroxylase(+) neurons in neonatal and adult mice. *J. Comp. Neurol.* 517, 37–50. <http://dx.doi.org/10.1002/cne.22132>.
- Yoon, K., Gaiano, N., 2005. Notch signaling in the mammalian central nervous system: insights from mouse mutants. *Nat. Neurosci.* 8, 709–715. <http://dx.doi.org/10.1038/nn1475>.
- Yu, X., Ng, C.P., Habacher, H., Roy, S., 2008. Foxj1 transcription factors are master regulators of the motile ciliogenic program. *Nat. Genet.* 40, 1445–1453. <http://dx.doi.org/10.1038/ng.263>.